2025

U.S. Department of Transportation
Federal Highway Administration

NEBRASKA
DEPARTMENT OF TRANSPORTATION

NEBRASKA
TRANSPORTATION CENTER

Final Report SPR-FY25(045)

Refined Analysis of Slab Bridges for Load Rating

Marc Maguire
Associate Professor
Durham School of Architectural Engineering and Construction
University of Nebraska-Lincoln

Jay Puckett
Professor Emeritus
Director
Durham School of Architectural Engineering and Construction
University of Nebraska-Lincoln

Nebraska Department of Transportation Research
Headquarters Address
1400 Nebraska Parkway
Lincoln, NE 68509
ndot.research@nebraska.gov
(402) 479-4697
https://dot.nebraska.gov/business-center/research/

Nebraska Transportation Center
262 Prem S. Paul Research Center at Whittier School
2200 Vine Street
Lincoln, NE 68583-0851
(402) 472-1932
http://ntc.unl.edu

This report was funded in part through grant from the U.S. Department of Transportation Federal Highway Administration. The views and opinions of the authors expressed herein do not necessarily state or reflect those of the U.S. Department of Transportation.

Technical Report Documentation Page

1. Report No. SPR-FY25(045)	2. Government Accession No.	3. Recipient's Catalog No.
4. Title and Subtitle Refined Analysis of Slab Bridges for Load Rating		5. Report Date December 2025
		6. Performing Organization Code
7. Author(s) Jay. A. Puckett, PE, PhD, F. ASCE Marc Maguire, PE, PhD		8. Performing Organization Report No. UNL- WBS 2611220155001
9. Performing Organization Name and Address University of Nebraska-Lincoln 1110 South 67th St. Omaha, Nebraska 68182-0178		10. Work Unit No.
		11. Contract SPR-FY25(045)
12. Sponsoring Agency Name and Address Nebraska Department of Transportation Research Section 1400 Hwy 2 Lincoln, NE 68502		13. Type of Report and Period Covered Final Report July 2024 – December 2025
		14. Sponsoring Agency Code

15. Supplementary Notes

16. Abstract

A finite element analysis application was developed to determine the live load distribution widths/factors for standard and non-standard axle configurations. This application will provide refined analysis to bridge rating engineers involved with load rating for inventory, operating, permits, and posting.

17. Key Words Structural analysis, slab bridges, finite element analysis, load rating, posting, permits, non-standard axles, barrier stiffness	18. Distribution Statement No restrictions. This document is available through the National Technical Information Service. 5285 Port Royal Road Springfield, VA 22161		
19. Security Classification (of this report) Unclassified	20. Security Classification (of this page) Unclassified	21. No. of Pages 172	22. Price

Form DOT F 1700.7 (8-72) Reproduction of completed page authorized

Table of Contents

List of Figures

List of Tables

Disclaimer

The contents of this report reflect the views of the authors, who are responsible for the facts and the accuracy of the information presented herein. The contents do not necessarily reflect the official views or policies of the Nebraska Department of Transportation or the University of Nebraska–Lincoln. This report does not constitute a standard, specification, or regulation. Trade or manufacturers' names, which may appear in this report, are cited only because they are considered essential to the objectives of the report.

The United States government and the State of Nebraska do not endorse products or manufacturers. This material is based upon work supported by the Federal Highway Administration under SPR-FY25(045). Any opinions, findings, and conclusions or recommendations expressed in this publication are those of the author(s) and do not necessarily reflect the views of the Federal Highway Administration.

This report has been reviewed by the Nebraska Transportation Center for grammar and context, formatting, and compliance with Section 508 of the Rehabilitation Act of 1973.

Abstract

NDOT has approximately 500 slab bridges in its inventory. These bridges frequently fail load rating procedures and super-load routing, leading to posting and operational limitations. This project develops a refined finite element analysis application to compute effective distribution widths for live load distribution. The refined analysis reduces conservatism inherent in AASHTO equations, thereby providing more accurate ratings and potentially eliminating postings. Non-standard and standard axle gages are considered.

Executive Summary

This project delivers a finite element application to evaluate slab bridges in Nebraska. The tool computes longitudinal bending moments and effective widths, validated against LRFD/LFD equations. Results can be imported directly into AASHTOWare Bridge Rating (BrR). A spreadsheet was developed to guide the engineer in linking the application and BrR. The tool improves NDOT's ability to rate slab bridges, allowing heavier vehicles to cross and minimizing unnecessary postings safely. The project tasks include application development, validation, implementation, training, and reporting. The long-term benefit is a modernized approach to bridge rating that better utilizes existing infrastructure.

Chapter 1 Background and Problem Statement

1.1 Background

NDOT has approximately 500 slab bridges in its inventory. These structures often fail to pass NDOT's load rating procedures and Superload automated Routing and Rating System that uses LARS/Superload and LFR to employ a beamline approach. Beamline analysis requires a distribution width *E* (the lane's width necessary to support one or two lanes of trucks). The load demands are inversely proportional to E, i.e., a refined finite element analysis (FEA) might increase E by 20%, so the load demand decreases by 20%. Better analysis can potentially economize bridge operations and allow vehicles to cross these structures safely. The process might allow for the increase or removal of posting signs for any posted structures.

The NDOT bridge rating operations are committed to the AASHTOWare Bridge Rating (BrR) software to rate the long-term storage of their inventory. NDOT's routing strategy uses a new version of Superload to access the BrR database. BrR has a publicly accessible application programming interface (API) to allow third-party developers access to the database to retrieve and place data.

Through in-service testing and refined analysis, research has shown that bridges may have significant reserve capacity due to various effects, e.g., stiffness of elements not considered in the design (concrete barriers and rails, curbs, integral piers, etc.). Azizinamini et al. (1998) extensively studied Nebraska's slab bridges, addressing field and laboratory testing, numerical modeling, and reliability analysis. This NDOR study provides a wealth of data compared to new modeling techniques. These researchers confirmed that reserve strength is typically significant. Two-dimensional (2D) shell finite element analysis represents the bridge deck as a continuous plate, directly capturing transverse and longitudinal distribution rather than through simplified strip approximations. This approach provides equivalent load distribution factors (LDFs)

consistent with system behavior, including shear lag, continuity, and stiffening from curbs and rails. Furthermore, 2D shell analysis enables explicit modeling of tire path loading, where concentrated wheel loads are tracked along realistic trajectories across the deck surface. This improves peak demand prediction in interior and exterior strips, addressing critical load cases that beamline methods only approximate. Therefore, a refined finite element approach is needed to provide NDOT with accurate, BrR-compatible rating tools.

1.2 Literature Review

1.2.1 Analytical Methods

Traditional analyses of slab bridges rely on simplified beamline models and effective-width approximations. The AASHTO Standard Specifications provided empirical distribution factors, while the LRFD Specifications (1994–present) introduced equations that better account for geometry and stiffness. These remain the basis for BrR. However, finite element analysis (FEA), increasingly used since the 1980s, captures shear lag, curb restraint, and redundancy more realistically, and aligns well with experimental data (Azizinamini et al., 1998; Zokaie, 2000; Eom & Nowak, 2001).

1.2.2 Experimental Testing

Field and laboratory testing consistently show that slab bridges perform better than predicted by simplified calculations. In Nebraska, UNL/NDOT studies in the 1990s demonstrated that measured live load distribution factors (LLDFs) were consistently lower than AASHTO predictions (Azizinamini et al., 1998).

Other DOTs reached similar conclusions. Ohio DOT field evaluations documented that integral curbs and railings provided significant edge stiffening, lowering measured strains in interior strips. Texas DOT studies on rural slab bridges confirmed that system behavior allowed greater effective width than prescribed by beamline methods, with reserve capacity evident even after cracking. Minnesota DOT conducted laboratory and field testing of slab-span systems, showing that continuity, flange thickness, and edge stiffening increased effective widths and reduced demand compared with AASHTO equations (Smith et al., 2005).

More recently, MnDOT and University of Minnesota researchers found that AASHTO ratings for slab-span bridges were often conservative; refined modeling and field testing produced rating factors up to 24% greater than code predictions (Dymond et al., 2023). Iowa DOT reported

similar outcomes in its bridge research program, where continuity and curb effects consistently reduced measured demands relative to design values (Iowa DOT, 2008). Virginia DOT also used refined 2D shell modeling validated against field data, confirming that effective widths and capacities were underestimated by simplified methods, and proposed regression-based adjustment factors for load rating (Harris et al., 2021).

Despite differences in span length, width, reinforcement details, and environmental conditions, these studies consistently reported that slab bridges exhibit greater effective widths, significant system redundancy, and reserve capacity masked by conservative formulas.

1.2.3 Role of Barrier Rails

Barrier rails, curbs, and parapets cast integrally with the slab act as stiff longitudinal members. Loads placed near the exterior can be shared with the rail, reducing demand on the slab and increasing effective width. This effect depends on rail condition—deteriorated or detached rails provide less benefit (Azizinamini et al., 1998; Conner & Huo, 2006). More recent field and FEA studies quantified these effects, showing that barriers substantially alter load paths, particularly for exterior loading, and should not be neglected in rigorous analysis (Hill, Dymond, Hedegaard, & Linderman, 2022).

A recent Indiana DOT–sponsored study conducted by Purdue University (SPR-4444, 2021) used 3D finite element parametric definitions for slab and T-beam bridges. The research varied rail heights and stiffness, showing increased exterior stiffness and reduced interior demand when rails were included. The effect was significant in slab bridges, and modification factors were proposed to adjust AASHTO distribution factors to account for rails, sidewalks, and parapets (Ravazdezh, Ramirez, and Haikal, 2021). While the formulations provide a systematic improvement, subsequent reviews noted that the scope was narrow (fixed geometry, linear

modeling assumptions) and that rail deterioration and transverse stress effects were not fully explored.

Several recent studies have extended rigorous analysis and testing of slab bridges. Hill (2022) conducted field load testing and FEA on slab-span bridges, confirming that AASHTO rating methods can be overly conservative and that barriers significantly influence distribution when loads are applied near the edge. A companion MnDOT/UMN study evaluated three slab-span bridges under calibrated truck loads, demonstrating that measured LLDFs were consistently lower than code predictions and that a calibrated plate model could improve rating accuracy (Hill, 2022; Hill et al., 2023). Here quantified barrier effects on slab-span bridges using 3D solid-element models, showing substantial changes in demand between exterior and interior strips. Together, these studies reinforce earlier observations of system redundancy, barrier stiffening, and conservatism in code formulas, and provide modern validation for incorporating rail and curb effects into rating methodologies.

Chapter 2 Objectives and Tasks

The primary objective of this project was to provide a method for computing refined effective widths for slab bridge load rating. A structural finite element application was developed to compute live load distribution widths, typically represented by the variable *E*; this width can be used to compute the live load distribution factor (LLDF) for a design/analysis strip. This application is called Slab Distribution Factor (SlabDF). A beamline analysis was combined with the LLDF to compute the load effect for the beamline.

Because slabs distribute live load well and the load effects are relatively small for live load shear, AASHTO does not require design or load rating checks for shear in slabs. Herein, the focus was on the bending moment in the span (M+) and near the interior supports (M-).

2.1 Objectives

- Develop a finite element application for slab bridges
- Compute effective widths for one- and two-lane loading
- Validate results with LRFD/LFD equations and other software
- Generate outputs for Slab DF, including 2-D and 3-D plots
- Demonstrate how to get data from SlabDF into AASHTOWare BrR
- Provide training and documentation

2.2 Tasks

The application was developed in an incremental process called interactive prototyping. Here, limited basic features are programmed and provided to clients earlier to gain input. Next generation prototypes were then programmed with more features, and again, input was solicited. Eight prototypes were reviewed to create the final deliverable.

1) Application Development Tasks

a) Develop a finite element application that analyzes slab bridges to determine the response, specifically longitudinal bending moments.

b) Use the response to compute and report effective widths.

c) Validate the application with static checks and comparisons with LRFD and LFD equations (AASHTO equations will be more conservative).

d) Write output graphics and reports that aid the validation of computations and permit checking.

2) Implementation Tasks

a) Document where the results may be entered into AASHTOWare BrR to create bridge/structure alternatives.

b) Demonstrate using the bridge alternative for different operational use cases.

c) Create a short video on the use of the application.

d) Provide a webinar to NDOT for engineers interested in using this application.

3) Write a final report.

4) Long-term and beyond scope – share findings with the bridge community.

Chapter 3 Application Development

3.1 Software Tasks

Software development tasks included:

1) Develop the structural model.
    a) Parametrically define the bridge geometry, material properties, loads, load positions, and analysis cross sections.
    b) Develop an analysis model using Comsol MultiPhysics ™, hereafter Comsol.
    c) Develop meshing strategies and studies.
    d) Conduct analysis and develop probes to log results for postprocessing.
    e) Develop postprocessing tools, including plot, equilibrium analysis, and integration tools for computing the effective widths.
2) Develop the User Interface.
    a) Develop a prototype user interface (UI) for NDOT review.
    b) Use the simple prototype to expose input parameters to the UI.
    c) Develop relationships between input parameters and bound limits for data checking.
    d) Develop a menu for execution and postprocessing.
    e) Develop multiple plot windows for 2- and 3-D plots.
    f) Develop input and output tables for all results, and next, develop simplified output tables.
    g) Develop output reports.
    h) Develop documentation, including examples, mesh studies, AASHTO spreadsheet for computations, beamline tool, etc.

3.2 Development tools

Comsol ™ has a tool to develop the user interface. The finite element tool and application development are tightly integrated and are unique to the industry. The Comsol tool is then used to compile the interface and the interface to the Comsol runtime modules, similar to almost all Windows applications that use Microsoft's runtime DLLs. The runtime can be

embedded into an executable application file (.exe), or the application can address a runtime downloaded separately. The end user does not have to purchase a Comsol license, and Comsol has no claim on these applications, royalties, etc. NDOT can share this application with their consultants and others as they wish.

NDOT will receive the base Comsol file (.mph). This file has all the information embedded for the parametric model and interface. NDOT must license the base Comsol and linear structural analysis module to use this file. Other modules are available, for example, nonlinear structures, geotechnical, computational fluid mechanics, etc. Details about Comsol can be reviewed at https://www.comsol.com/. Various modules are shown at https://www.comsol.com/products. Many videos are at https://www.comsol.com/products

3.3 Parametric Definition of the Slab Bridge Model

The slab bridge model uses a fully parametric framework to allow systematic variation of geometry, material properties, and loading conditions. This enables efficient generation of multiple configurations for sensitivity studies and rating evaluations.

Figure 3.1 provides the parametric definition of the bridge. Figure 3.2 provides the geometry for the optional barrier rail stiffness.

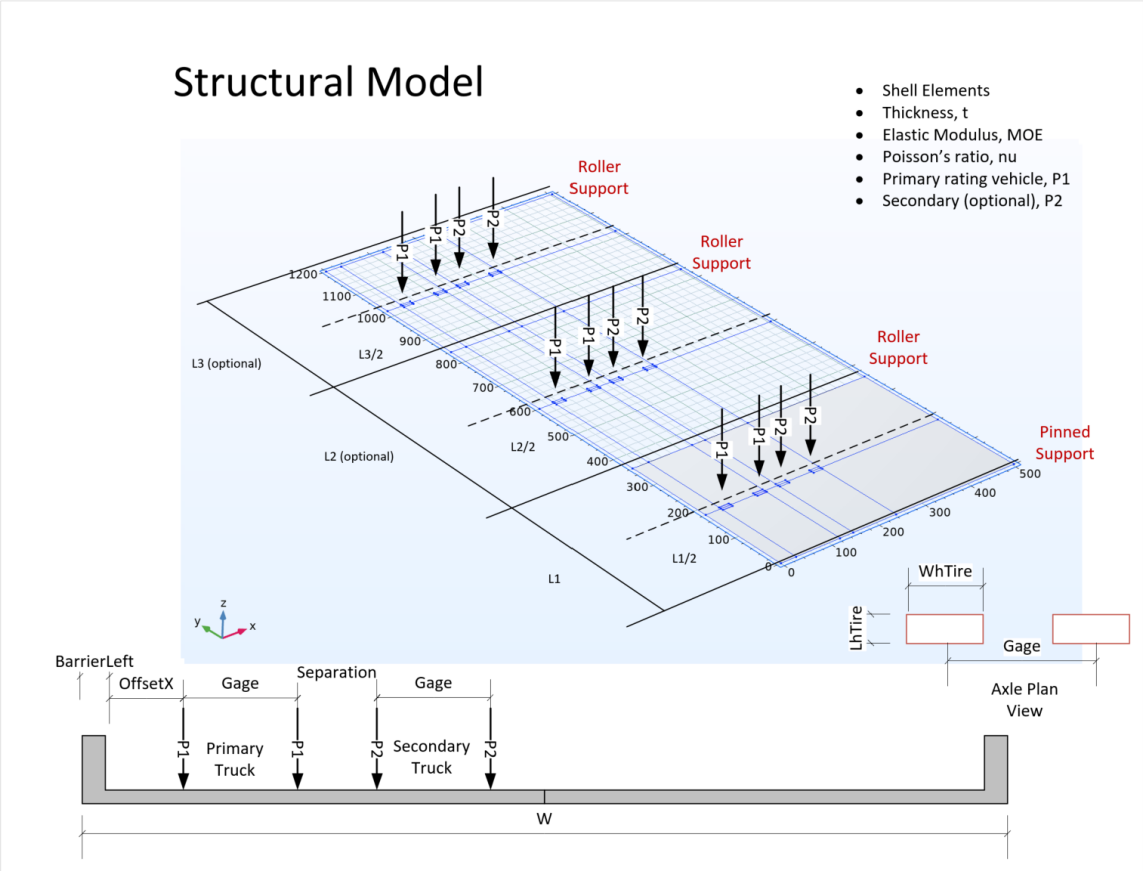

Figure 3.1 Parametric Model

Parameters include the following:

Elements: The deck is discretized using quadrilateral shell elements with specified thickness (*t*).

Material Properties: Elastic modulus (*MOE*) and Poisson's ratio (ν) define linear elastic behavior.

Supports: Pin and roller supports are placed on the transverse edges. This ensures stable boundary conditions while allowing realistic deformation.

Span Lengths (L1, L2, L3): The longitudinal span (L1) defines the primary direction of load transfer. Optional spans (L2, L3) can be included to capture multi-span effects.

Bridge Width (W): The transverse dimension, including barriers, defines the total edge-to-edge width.

Offsets and Barrier Positions: Parameters such as BarrierLeft and OffsetX locate curb and barrier positions relative to the loaded lanes.

Primary Vehicle (P1): The main rating truck is modeled as discrete wheel loads applied along prescribed tire paths.

Secondary Vehicle (P2): An optional second truck can be added to represent multiple-lane loading or permit scenarios.

Axle Parameters: Loads are positioned by specifying:

3) WhTire (tire patch width)
4) LtTire (tire patch length)
5) Gage (wheel line separation)
6) Separation (longitudinal distance between right wheel on P1 and left wheel on P2)

OffsetX: By adjusting offset parameters, wheel loads can be shifted laterally across the bridge to evaluate critical load positions

Rail (barrier) Parametric Model:

- Area, A_{xx}
- Moment of inertia, I_{zz}
- Moment of inertia, I_{yy}
- Torsional constant, J_x
- Eccentricity, e (distance from the midsurface of the deck to the rail centroid

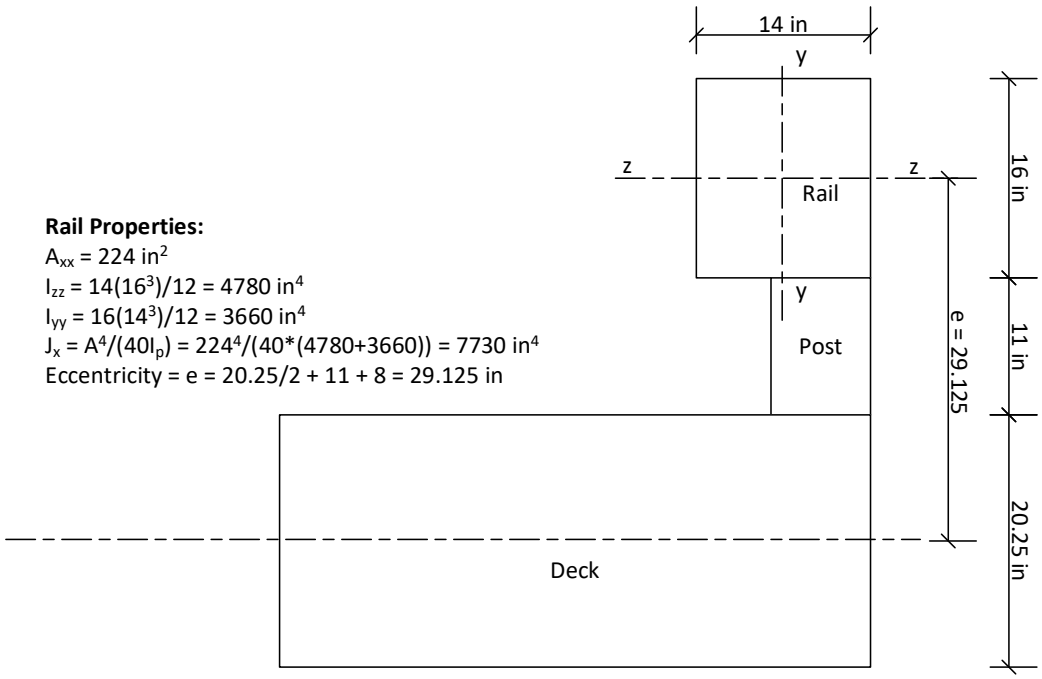

Figure 3.2 Rail Geometry and Properties

3.3.1 Parametric Capabilities

The framework allows:

- Rapid span length, width, and slab thickness variation to match bridge inventory ranges;
- Direct study of barrier effects by toggling the barrier offset and stiffness properties;
- Systematic application of truck loading patterns, enabling evaluation of interior vs. exterior strips under realistic tire paths; and
- Expansion to multi-lane or tandem trucks by adjusting gage and separation inputs.

3.3.2 Slab DF Interface Overview

The base screen is illustrated in Figure 3.3. Along the left side is the input area. Here, the parameters exposed to the user are listed. Fields are checked for input bounds and the relationship between variables. Along the top is a robust menu system divided into the following sections:

- Starters
  - Update geometry
  - Plot mesh
- Simulation
  - Compute model
  - Clear solutions
- Mxx Results 3-D
  - Mxx Position 1
  - Mxx Position 2
  - Mxx Position 3
  - Translations Position 1
  - Translations Position 2
  - Translations Position 3
- Mxx Results 2-D
  - Midspan Position 1
  - Midspan Position 2
  - Midspan Position 3

- Translation Results 2-D
    - Midspan Position 1
    - Midspan Position 2
    - Midspan Position 3

- Write report

- Miscellaneous
    - Graphics tool help
    - Application manual (to be the narrative for Example 1)
    - AASHTO 4.6.2.3
    - Research Proposal (to be removed)
    - Mesh study
    - Excel spreadsheet
    - Continuous beam tool
    - Example
        - One-span
        - Two-span
        - Three-span
        - Non-standard gage
        - Using results in BrR

- Ender
    - Reset windows
    - Exit application

The largest portion of the screen is dedicated to the output display, where the following graphics are available:

- Graphics
    - 2- and 3-D graphics are presented here

- Reactions
    - Shows a reaction table

- Detailed Input
    - Echoes input from the engine – ensures that the engine is getting intended values

- Detailed Computations
    - Provides detailed and large tables containing all the intermediate data so the summary data can be validated

- Summary
    - Provides the most important results that can be put into BrR

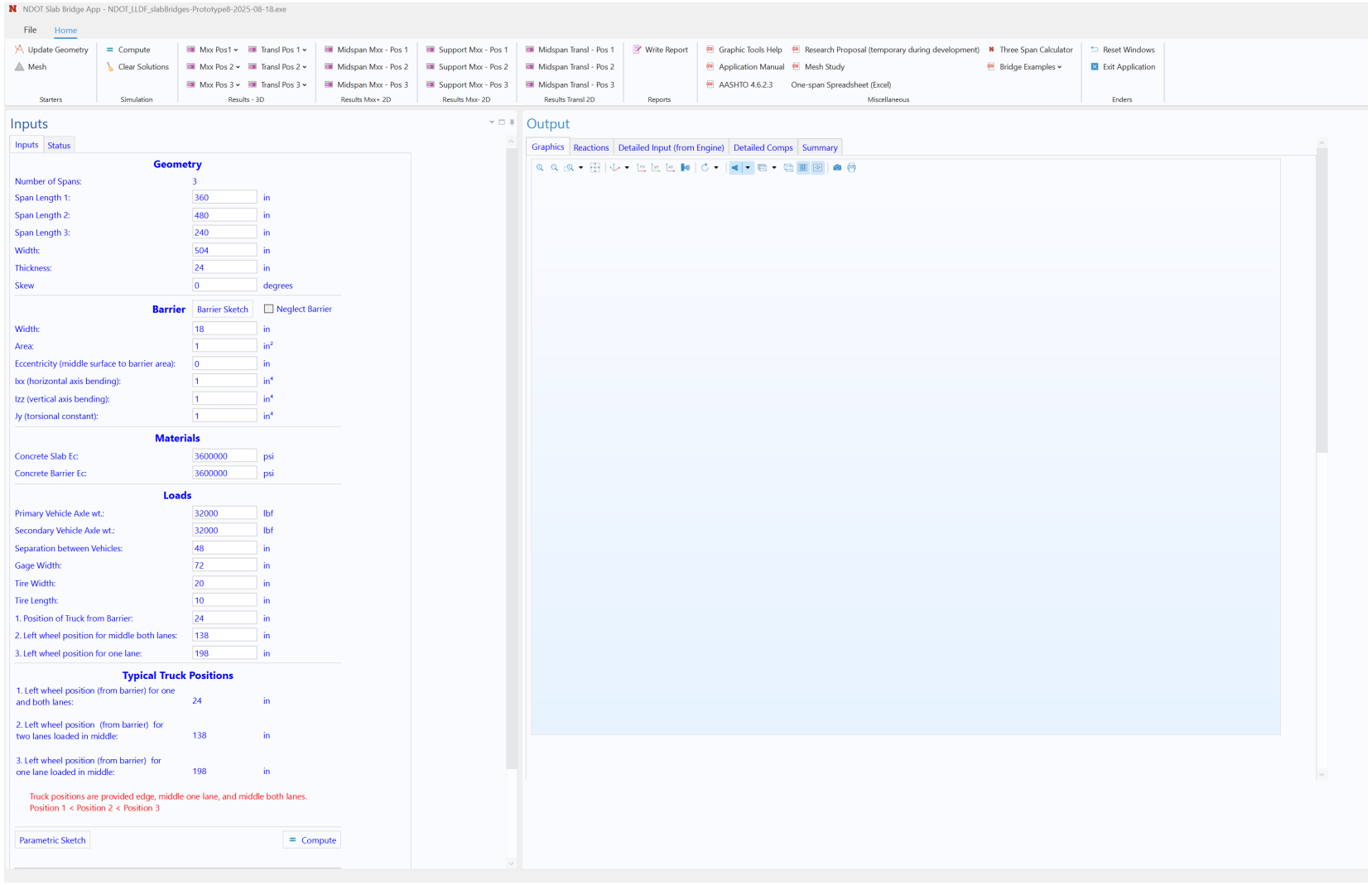

Figure 3.3 Slab DF Interface

3.3.3 Finite Element Details

Shell elements are free isotropic quadrilaterals of uniform thickness *t*. The material properties are the modulus of elasticity *E* and Poisson's ratio ν. The reinforcement is not modeled. The shape function is quadratic. The solver is linear elastic and static. The load is uniformly applied to the wheel patch. The wheel loads and patch dimensions are defined by the user, so the load per area is applied. The number of spans is determined based on the number of span lengths entered (three spans maximum). Three spans were selected for simplicity of programming in COMSOL. Bridges with more than three spans can be modeled with different respective span lengths. The important behavior to capture is the end span with one continuous support and the middle span with two continuous supports. A typical mesh is shown in Figure 3.4.

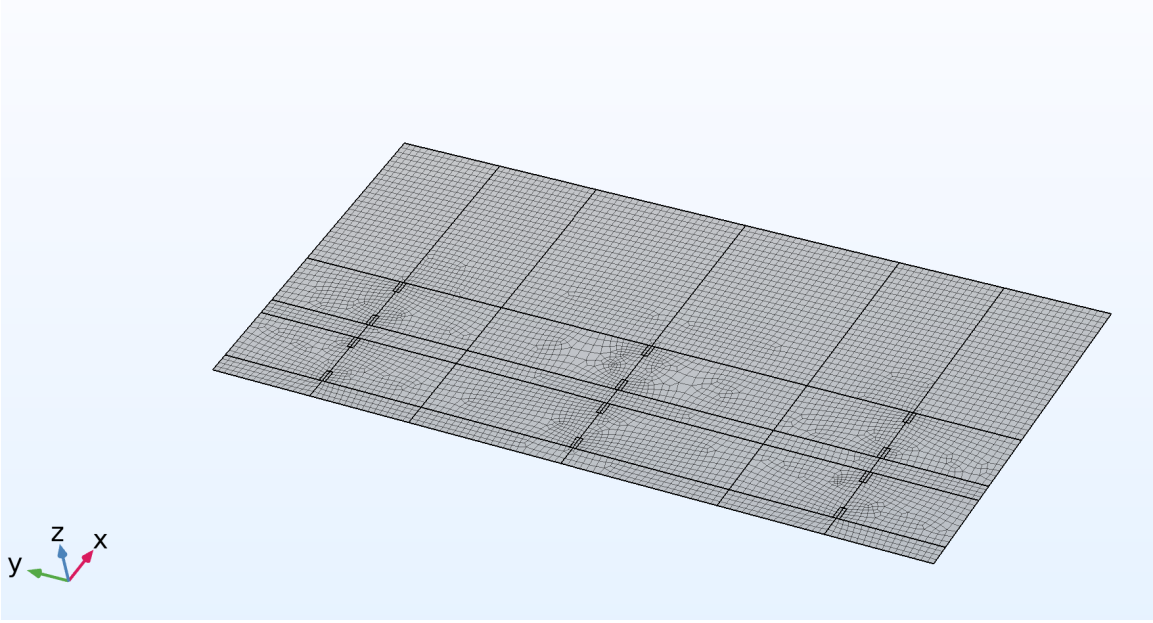

Figure 3.4 A Typical Mesh SlabDF

3.3.4 Mesh Study

A series of meshes was used to model a one-span slab bridge with two lanes loaded (see Table 3.1). For this simulation, coarse meshes provided the same results as fine meshes. The element employs a Quadratic Lagrange shape function. Essentially, all meshes provided the same results for distribution width. The details of the study are provided in Appendix E.

Table 3.1 Summary Simulations with Different Meshes

Mesh	Nominal Element size, in	DOFs	Solution Time, sec
1	20	27150	2
2	10	78438	5
3	2	1472094	32

3.4 Effective Width Computations

The effective slab width is computed based on the bending moment under the load (a transverse line). This moment M_{xx} has units of length x force / length, for ft-kip/ft, or kip. Integrating the moment along this line provides the equilibrium moment for the entire bridge, M_{total}. Figure 3.5 shows the plot for M_{xx}. Note the moments are larger under the loads as expected. Away from the load, the moments decrease. The effective width attempts to determine the average moment under the load. This is not necessarily the maximum, but a reasonable value that might be used for design. The moment in the loaded region is determined by numerically integrating the moment function under the load (see Figure 3.6). This region is located within the outer edges of the wheel patches for one vehicle. The effective width E is the ratio of the equilibrium moment and the moment under load. The LLDF is determined by dividing the analysis strip by the effective width. This factor is then used in the beamline analysis (typically performed in AASHTOWare ™ Bridge Rating (BrR).

Note that the equilibrium moment may be independent of SlabDF, for example, by statics, PL/4 for a simple beam. A continuous beam analysis is required for multiple spans. Typically, hand computations and numerical integration for the equilibrium moment are within two percent.

These computations are demonstrated in numerous examples presented later in this report.

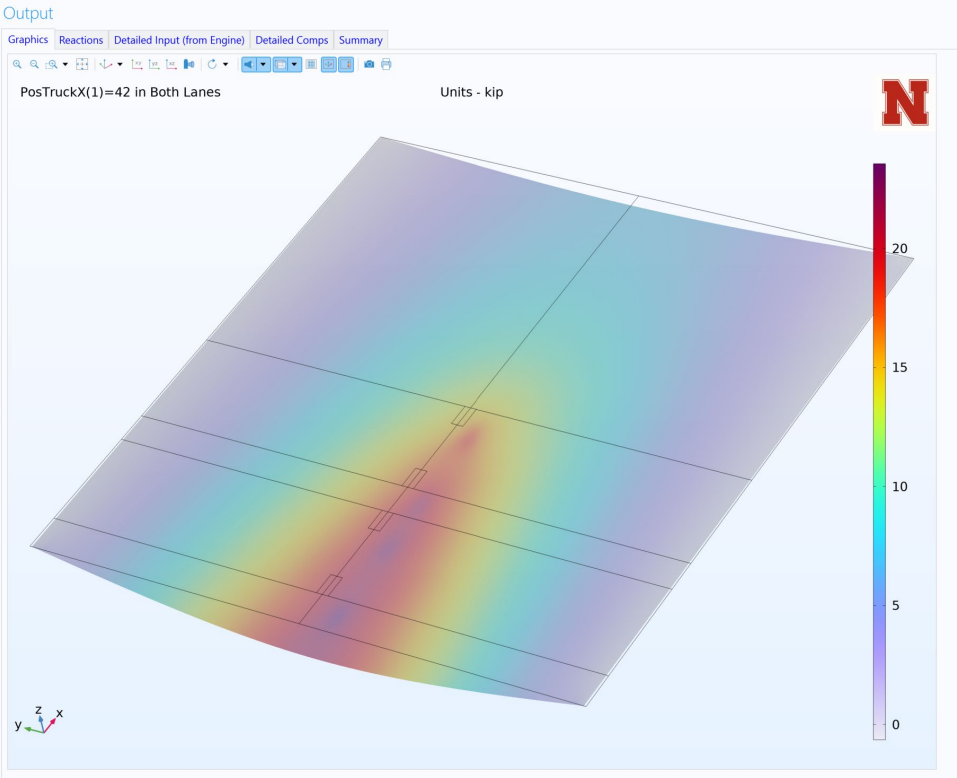

Figure 3.5 One-span slab loaded with two lanes near the edge

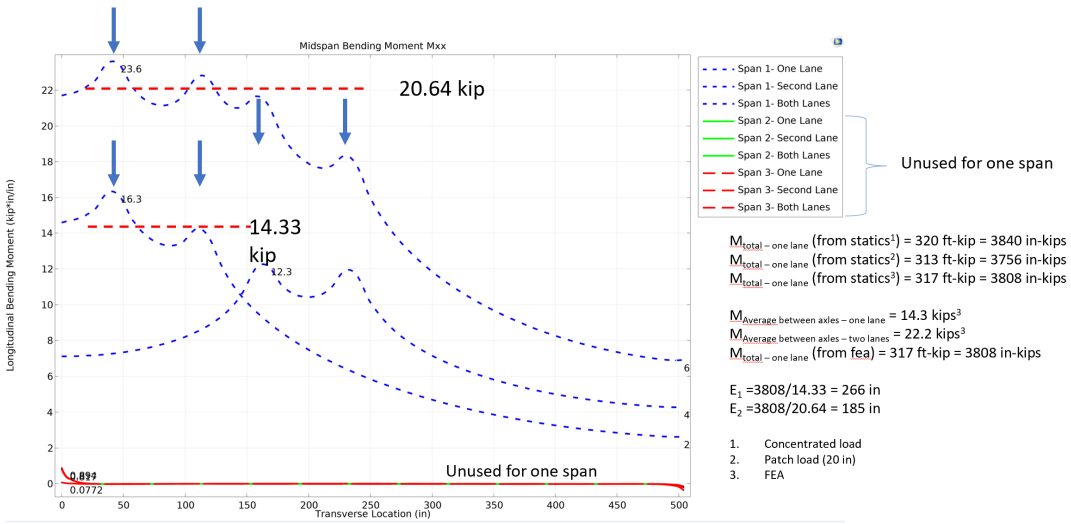

Figure 3.6 Bending moment along the transverse section under the loads

3.4.1 AASHTO 4.6.2.3

AASHTO-LRFD 4.6.2.3 provides effective width equations for loaded one and two-lane bridges (see Figure 3.7). This short section is provided for convenience.

factor

4.6.2.3—Equivalent Strip Widths for Slab-Type Bridges

C4.6.2.3

This Article shall be applied to the types of cross-sections shown schematically in Table 4.6.2.3-1. For the purpose of this Article, cast-in-place voided slab bridges may be considered as slab bridges.

The equivalent width of longitudinal strips per lane for both shear and moment with one lane, i.e., two lines of wheels, loaded may be determined as:

$$E = 10.0 + 5.0\sqrt{L_1 W_1} \qquad (4.6.2.3\text{-}1)$$

In Eq. 4.6.2.3-1, the strip width has been divided by 1.20 to account for the multiple presence effect.

The equivalent width of longitudinal strips per lane for both shear and moment with more than one lane loaded may be determined as:

$$E = 84.0 + 1.44\sqrt{L_1 W_1} \le \frac{12.0W}{N_L} \qquad (4.6.2.3\text{-}2)$$

where:

E = equivalent width (in.)
L_1 = modified span length taken equal to the lesser of the actual span or 60.0 (ft)
W_1 = modified edge-to-edge width of bridge taken to be equal to the lesser of the actual width or 60.0 for multilane loading, or 30.0 for single-lane loading (ft)
W = physical edge-to-edge width of bridge (ft)
N_L = number of design lanes as specified in Article 3.6.1.1.1

For skewed bridges, the longitudinal force effects may be reduced by the factor, r:

$$r = 1.05 - 0.25\tan\theta \le 1.00 \qquad (4.6.2.3\text{-}3)$$

where:

θ = skew angle (degrees)

Figure 3.7 AASHTO 4.6.2.3

3.4.2 Barrier Rail Stiffness

The barrier rail is modeled with a beam element located at an eccentricity e, which positions the beam centroid relative to the middle surface of the shell elements. This numerically accounts for the "parallel axis" effect.

Including the barrier stiffness is optional, and excluding it is conservative. Examples are provided later to compare analyses with and without consideration of this stiffness.

3.4.3 Load Cases

Loads are positioned in the middle of each span. The transverse positioning defaults to three cases:

a) Load group is positioned as close to the edge as possible (within two feet of the travelway edge).

b) Load group is positioned so that the left lane is in the middle of the bridge.

c) Load group is positioned so that the centroid of both lanes is in the middle of the bridge.

For each load position, one- and two-lane load cases are computed, separately and combined. These default positions are provided for convenience and may be changed by the user. Permit vehicles with non-standard axles can be modeled by setting the axle gage and separation distance to model four wheels. An example is illustrated later in this report.

3.5 Continuous Beamline Tool

To aid the engineer in checking equilibrium, a beamline tool was created and linked into SlabDF. Figure 3.8 illustrates the input and output. The loading is the same as the FEA analysis, so the check compares the FEA total section moments, $M_{total,}$ with the beamline moments. Any differences should be within a few percent.

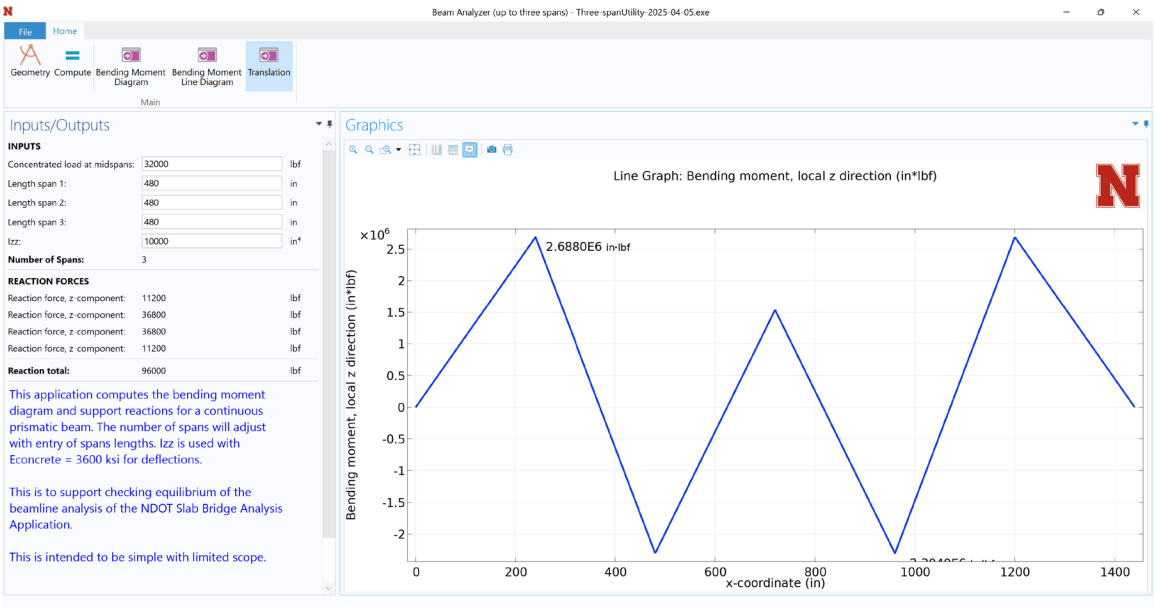

Figure 3.8 Beamline tool

3.6 Excel Spreadsheet for AASHTO Effective Width Computations

An Excel spreadsheet was developed to compute the AASHTO effective width per AASHTO-LRFD 4.6.2.3. This sheet was provided and linked to SlabDF for the engineer's convenience. A screenshot is provided in Figure 3.9. This is the baseline case for the finite element analysis provided in Chapter 4. (L = 40 ft, W = 42 ft, Skew = 0) This provides additional checks on the reasonableness of FEA results. An additional tab sheet was provided to compute the moment due to a uniform load to aid in defining points of contraflexure in BrR.

Slab Bridge AASHTO Computations			
Abstract: This spreadsheet computed AASHTO effective widths for slab bridges. The specification reference is provided.			
Date:	4/29/2025		
Variable	**Value**	**Units**	**Comments**
P =	*32*	kip	Axle load
L =	*40*	ft	Span length (compute for each span)
M (LL approx) =	*320*	ft-kips	Simple-beam moment
M (LL approx) =	*3840*	in-kips	Simple-beam moment
W =	*42*	ft	Slab width
t =	*14*	in	Slab thickness
θ =	*10*	degrees	Skew Angle
BarrierWidth =	*22*	in	Barrier Width
Strip width =	*112*	in	
Middle Strip Computations			
Skew Factor =	1.000		
NL	1		Number of lanes loaded
L1 =	40	ft	min(L,60)
W1 =	30	ft	min(30, W)
E1 (Formula) =	183.21	in	Eq. 4.6.2.3-1
E1/SkewFactor =	183.2	in	Skew adjustment decreases load effect
LLDF =	**0.005**		Distribution factor of one-in section
LLDF x strip width	**0.611**	Lanes	
M1 =	1.7	kips-in/in	Required resistance
M1 =	21.0	kips-in/ft	
NL	2		More than one lane loaded
L1 =	40	ft	min(L,60)
W1 =	42.0	ft	See specifications
E2 (Formula) =	143.0	in	Eq. 4.6.2.3-2
E2 max =	252.0	in	12*W/NL
E2 =	143.0	in	min(E2max, E2)
E2/SkewFactor =	143.0	in	Skew adjustment decreases load effect
LLDF =	**0.007**		
LLDF x strip width	**0.783**	Lanes	
M2 =	2.2	kips	Static moment/effective width
M2 =	26.8	kips-in/ft	
Edge Strip Computations			
Barrier width =	22.00	in	Distance from edge of deck to edge of barrier
One foot per spec	12.00	in	See spec
1/4 for strip width =	549.62	in	See spec
Subtotal =	583.62	in	Total
1/2 of strip width =	1099.23	in	See spec
Max 72	72.00	in	See spec
Edge Strip Width =	72.00	in	Check minimum
Edge Strip Width =	6.00	ft	Per spec, this is for one wheel line 1/2 axle
LLDFwheelLine=	0.167		For wheel line
LLDFperLane=	**0.083**		For lane

Figure 3.9 Spreadsheet for AASHTO Computations

Chapter 4 Slab Bridge Validation Example

4.1 Introduction

Rigorous finite element analysis (FEA) is increasingly used in rating and evaluating slab-type highway bridges. Although AASHTO LRFD specifications provide approximate methods for load distribution, these equations were developed primarily for design. They may not always reflect the actual behavior of existing bridges under rating scenarios. To ensure reliability of advanced analysis tools, it is important to benchmark them against fundamental statics and recognized design equations.

This section presents a one-span slab bridge validation study. The example is a 40-ft span reinforced concrete slab subjected to wheel loads. By examining this representative but straightforward case, the study demonstrates how FEA aligns with hand-calculated statics, quantifies live load distribution factors (LLDFs), and assesses the influence of skew and barrier stiffness. The findings illustrate that advanced methods can be applied confidently and provide additional insights beyond simplified equations.

4.2 Model Definition and Assumptions

The base finite element model was established with the following characteristics:

Support conditions: Simple supports at both ends.

- Slab geometry: Uniform thickness with no barrier stiffness in the base case.
- Load definition: Wheel patch loads of 16 kips, applied as uniform pressures over the tire footprints.
- Lane cases: One-lane and two-lane loading considered.
- Evaluation section: Moments extracted across gage widths plus wheel footprints.

These assumptions replicate standard load rating conditions while allowing for incremental inclusion of effects such as skew and barrier stiffness. Figure 4.1 shows the parametric geometry and load application. Some figures are repeated, so this example is standalone. Figure 4.2 shows

the mesh with notations for the one-span example. Note that the optional barrier frame element will be used to extend this base example.

Table 4.1 provides the parameter data.

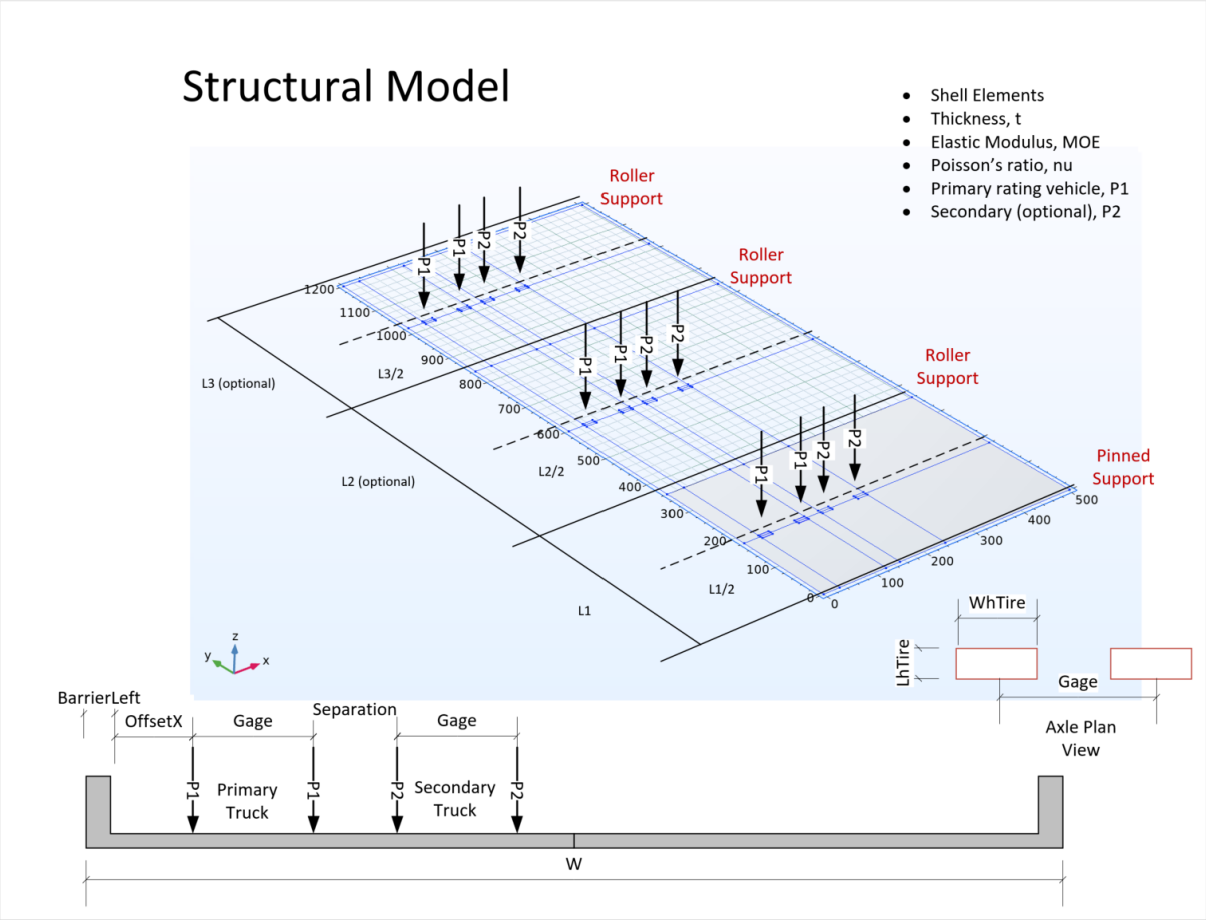

Figure 4.1 Parametric model definition (provided here for convenience reference)

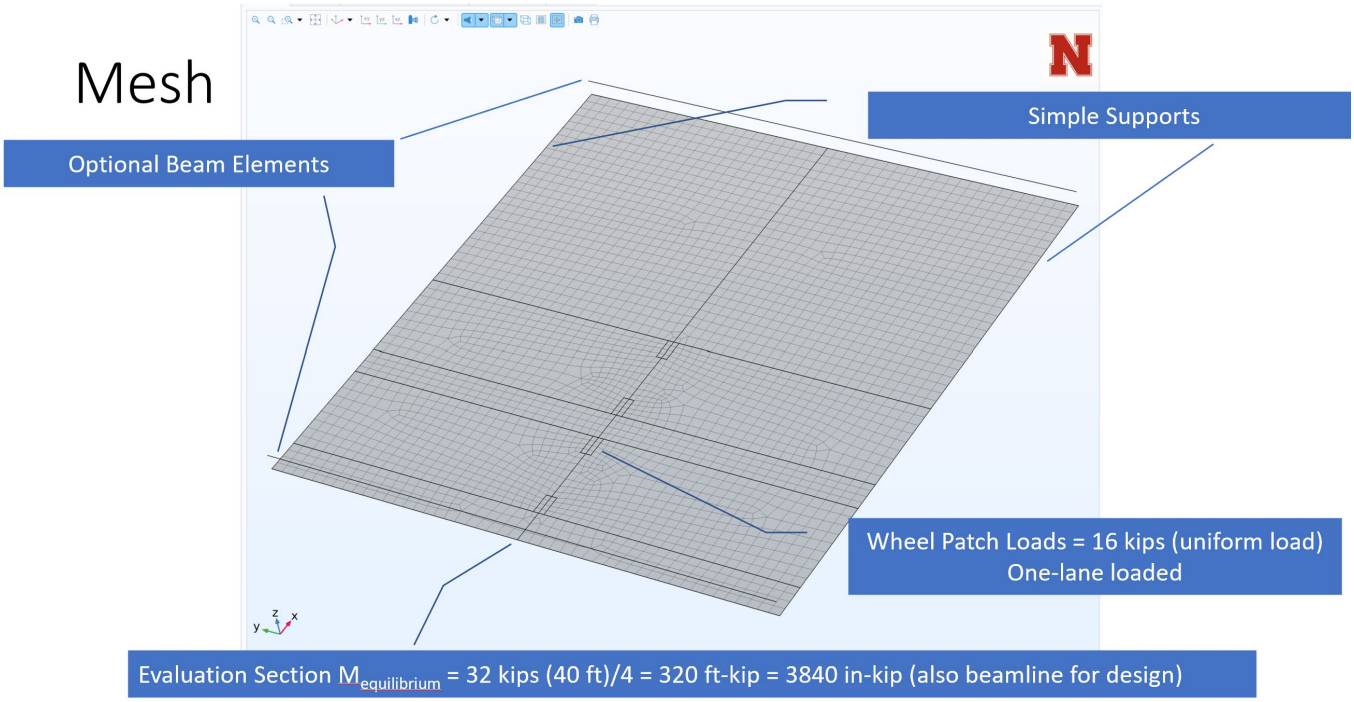

Figure 4.2 Mesh with notations

Table 4.1 Example parameters

Parameter	Value
Span 1 Length	40 ft (one-span bridge)
Width	42 ft
Thickness	18 in
Wheel load	16 kips
Edge truck position from edge of travelway	24 in
Truck gage	72 in
Truck separation	48 in
Tire width	20 in
Tire length	10 in
Left barrier width	18 in
Right barrier width	18 in
Barrier stiffness	Ignore
Skew	0 degrees

4.3 Static Validation

A concentrated 32-kip load was applied at midspan to confirm equilibrium, and the beamline reactions were computed. The resulting bending moment was 320 ft-kip. When distributed as a 20x10-in. patch load, the moment reduced slightly to 313.3 ft-kip.

The finite element model accurately reproduced this behavior, with FEA-calculated midspan moments of 317 ft-kip (from integrating the shell bending moments, M_{xx}). This close agreement between statics and FEA, within ±2%, is an important validation, instilling confidence in the model's numerical stability and physical consistency (see Figure 4.3).

Support reactions are provided in the output (see Figure 4.4) where the reactions are symmetrical and add to the applied loads. This symmetrical and additive nature of the support

reactions is a fundamental result checking process that should be rigorously followed for all bridges studied.

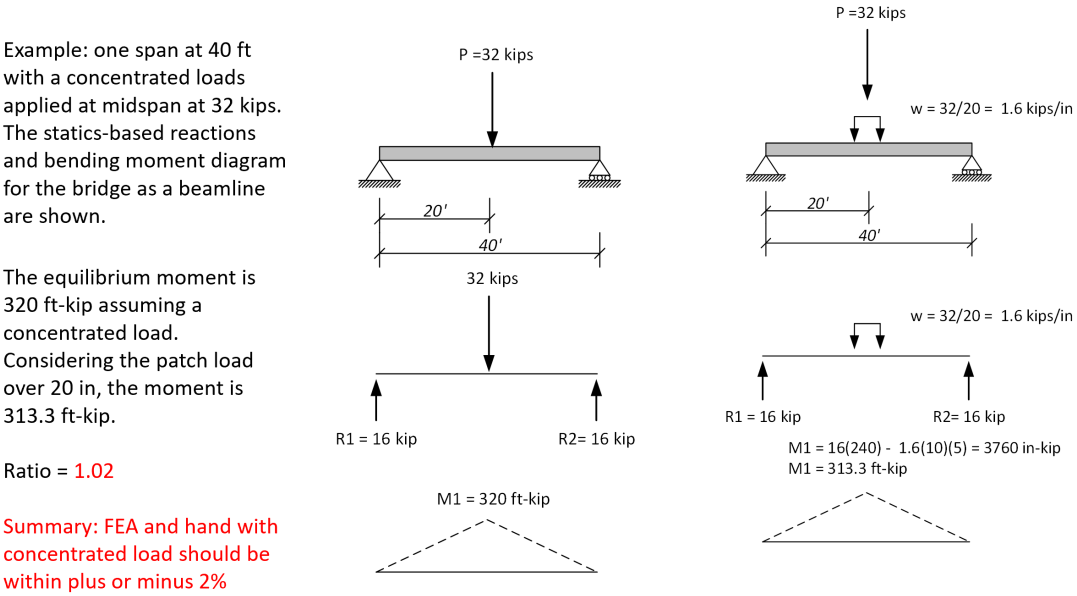

Figure 4.3 Statics check

Output

Graphics | Reactions | Detailed Input (from Engine) | Detailed Comps | Summary

Reactions

Reactions

PosTruckX (in)	42.000	42.000	42.000	156.00	156.00	156.00	216.00	216.00	216.00
loadcase	1.0000	2.0000	3.0000	1.0000	2.0000	3.0000	1.0000	2.0000	3.0000
group.One_Lane_Loaded	1.0000	0.0000	1.0000	1.0000	0.0000	1.0000	1.0000	0.0000	1.0000
group.Second_Lane_Loaded	0.0000	1.0000	1.0000	0.0000	1.0000	1.0000	0.0000	1.0000	1.0000
Reaction 1 (kip) (lbf)	16.000	16.000	32.000	16.000	16.000	32.000	16.000	16.000	32.000
Reaction 2 (kip) (lbf)	16.000	16.000	32.000	16.000	16.000	32.000	16.000	16.000	32.000
Reaction 3 (kip) (lbf)	0.0000	0.0000	0.0000	0.0000	0.0000	0.0000	0.0000	0.0000	0.0000
Reaction 4 (kip) (lbf)	0.0000	0.0000	0.0000	0.0000	0.0000	0.0000	0.0000	0.0000	0.0000
Rtotal (kip) (lbf)	32.000	32.000	64.000	32.000	32.000	64.000	32.000	32.000	64.000

Figure 4.4 Reaction output

4.4 Finite Element Results – Base Case

Under edge lane loading, the slab experienced maximum sectional moments of 16.3 kips for one-lane loading and 23.6 kips for two-lane loading. These values reflect the expected superposition of live load effects as additional lanes are engaged. Midspan deflections increased, underscoring the model's ability to capture realistic behavior.

The distribution of stresses across the evaluation section revealed concentration near the loaded wheel paths, gradually diffusing into the slab as the load transferred transversely. Figure 4.5 illustrates the moment "heatmap", highlighting how FEA captures realistic slab behavior beyond one-dimensional beamline assumptions.

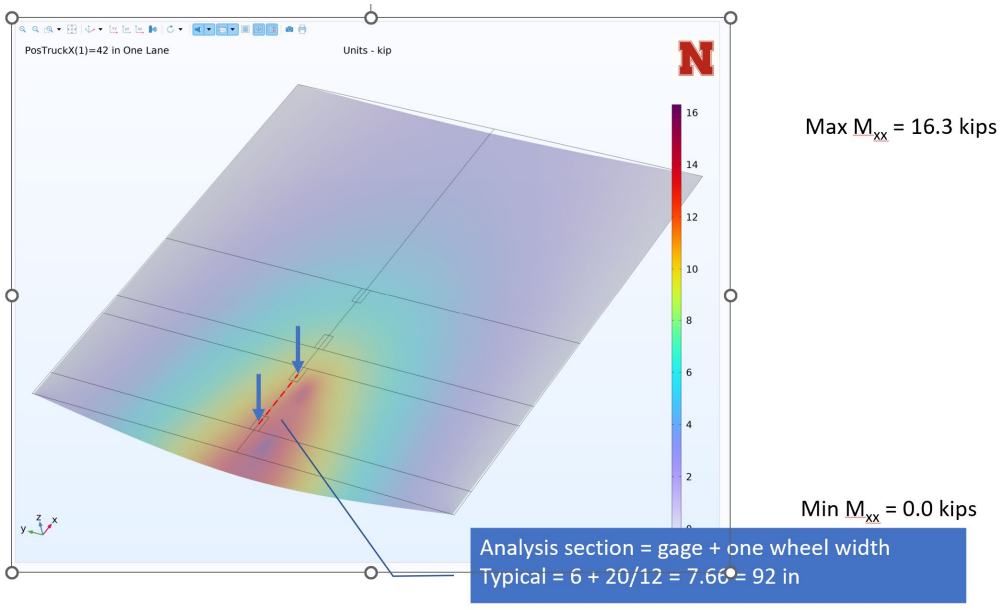

Figure 4.5 One lane is loaded near the edge

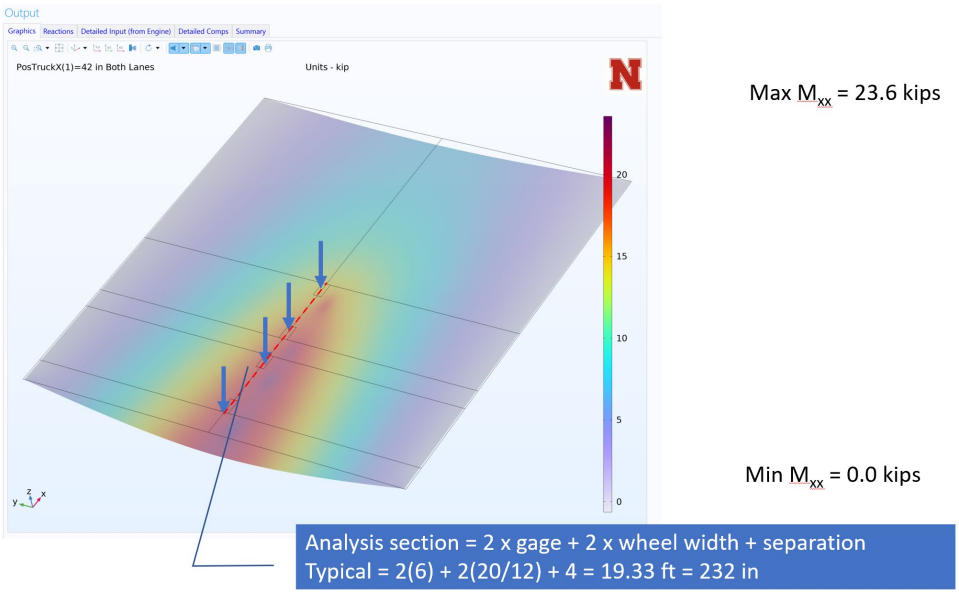

Figure 4.6 Two lanes are loaded near the edge

4.5 Live Load Distribution (LLDF) – Edge Loading

Live load distribution factors were calculated by dividing the total applied moment by the average sectional moment across the slab width. For one-lane loading, the effective width E1 was 266, corresponding to an LLDF of 0.045. For two-lane loading, E2 was 185 in, and LLDF was 0.065. LLDFs are based on a 1-ft analysis strip. These can be adjusted for other analysis strip widths by linear proportioning. See Figure 4.7.

The three load positions are illustrated: 1. left-most lane, 2. right-most lane, and 3. both lanes. For these cases, 1 and 3 will be of interest (critical). The maximum moments are shown as 16.3 kip-ft/ft and 23.6 kip-ft/ft. The numerically integrated averages are 14.33 kip-ft/ft and 20.64 kip-ft/ft. The effective width computations are provided. The LLDFs are computed by: 12/185 = 0.065 and 12/266 = 0.045 for one- and two-lanes, respectively.

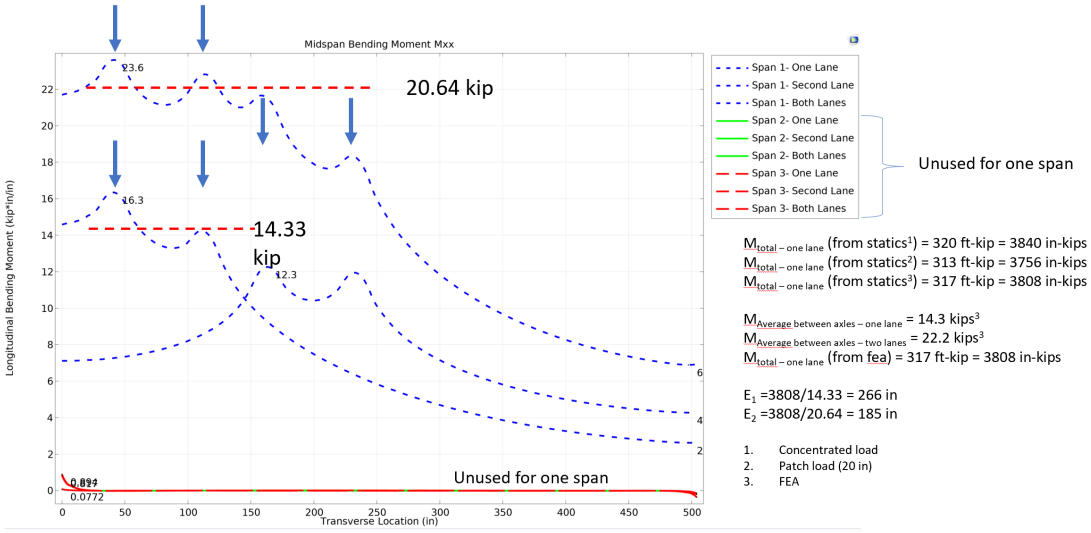

Figure 4.7 Bending moments plotted across the transverse section near the edge

These results compare favorably with AASHTO provisions, which prescribe effective widths between 183 and 220 inches for similar spans. The alignment confirms that FEA and code-based methods produce comparable outcomes under standard configurations (see Figure 4.7). $E_{1AASHTO}$ = 183 in, $E_{1AASHTO}$ (without MFP) = 220 in, and $E_{2AASHTO}$ = 143; the FEA values differ by about 20 percent for edge loading. Note that the AASHTO equations were calibrated for the edge loading.

4.6 Effective Width – Central Loading

Figure 4.8 illustrates one lane positioned in the middle of the bridge. Figure 4.9 provides the bending moments. The one-lane loaded position is of typical interest for this position. Transverse participation increased when the lane was placed in the middle of the slab. The average moment across the section dropped to 11.0 kips, yielding an effective width of 346 in. and LLDF = 0.035. This effective width ratio with $E_{1AASHTO}$ (without MFP) = 220 in provides (346/220) = 1.76, a significant increase in width and decrease in load effect.

This finding emphasizes the sensitivity of effective width to load position. Central placement engages more of the slab in flexure, while edge placement limits participation due to the edge being free to flex transversely. For design purposes, this behavior justifies using different LLDF values for edge and interior positions, a distinction consistent with AASHTO equations.

The position with two lanes in a central position is provided in the appendix for a complete PowerPoint deck.

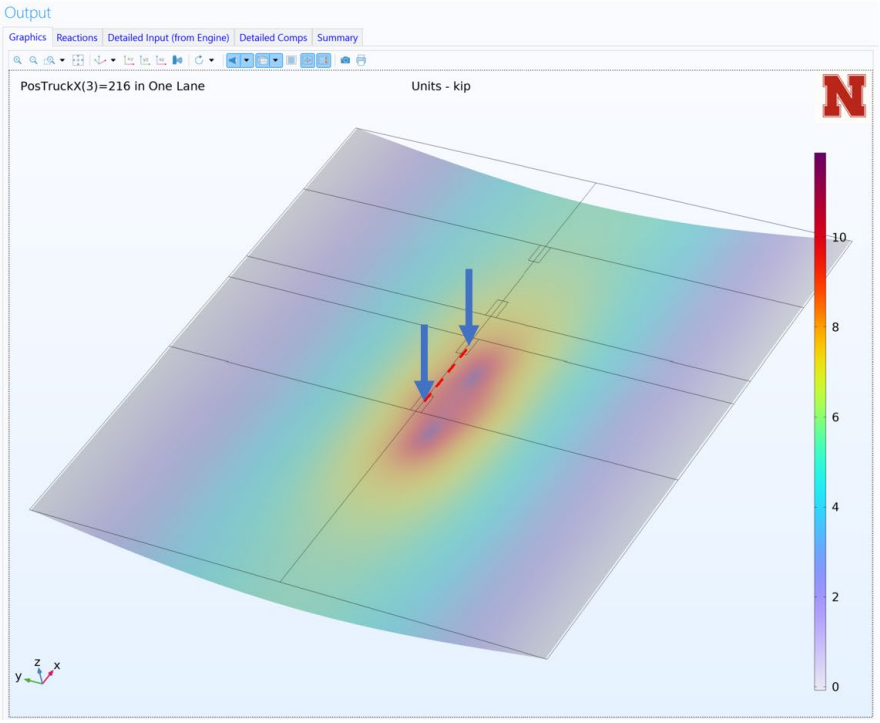

Figure 4.8 One-lane load positioned centrally

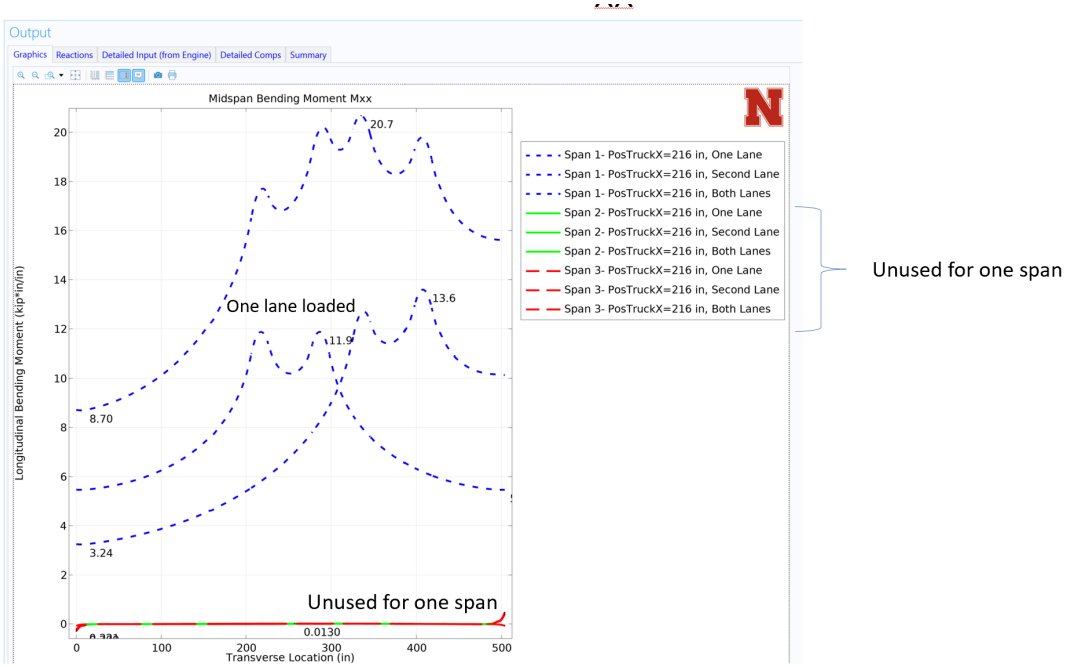

Figure 4.9 Bending moment for one lane position centrally

4.7 AASHTO Equations and Skew Effects

Bridges with skewed support often display a non-uniform distribution, with one corner of the span attracting higher forces. The base study was expanded to use a 30° skew. AASHTO specifies a skew reduction factor of approximately 0.9 for such conditions. The FEA results confirmed this reduction, showing effective widths approximately 10% smaller than the unskewed case. In SlabDF, the AASHTO equation is used and automatically applied. See Figure 4.10 for AASHTO 4.6.2.3.

Figure 4.10 illustrates the typical SlabDF output. The AASHTO computations are at the top, and the FEA results are at the bottom. These tables are provided for all SlabDF analyses.

Skew Factor Computation

Output

Graphics | Reactions | Detailed Input (from Engine) | Detailed Comps | Summary

Detailed Computations Summary

AASHTO

PosTruckX (in)	42.000	42.000	42.000	156.00	156.00	156.00	216.00	216.00	216.00
loadcase	1.0000	2.0000	3.0000	1.0000	2.0000	3.0000	1.0000	2.0000	3.0000
group.One_Lane_Loaded	1.0000	0.0000	1.0000	1.0000	0.0000	1.0000	1.0000	0.0000	1.0000
group.Second_Lane_Loaded	0.0000	1.0000	1.0000	0.0000	1.0000	1.0000	0.0000	1.0000	1.0000
E1 from AASHTO Eq. (in)	183.21	183.21	183.21	183.21	183.21	183.21	183.21	183.21	183.21
E1 from AASHTO Eq with m=1.2 removed (in)	219.85	219.85	219.85	219.85	219.85	219.85	219.85	219.85	219.85
E2 from AASHTO Eq. (in)	143.02	143.02	143.02	143.02	143.02	143.02	143.02	143.02	143.02
Skew Correction Factor	0.90566	0.90566	0.90566	0.90566	0.90566	0.90566	0.90566	0.90566	0.90566
E1 (net) from AASHTO Eq. (in)	202.29	202.29	202.29	202.29	202.29	202.29	202.29	202.29	202.29
E1 (net) from AASHTO Eq. with m=1.2 removed (in)	242.75	242.75	242.75	242.75	242.75	242.75	242.75	242.75	242.75
E2 (net) from AASHTO Eq. (in)	157.92	157.92	157.92	157.92	157.92	157.92	157.92	157.92	157.92
LLDF One Lane (per ft) (1)	0.059321	0.059321	0.059321	0.059321	0.059321	0.059321	0.059321	0.059321	0.059321
LLDF One Lane (no m=1.2) (per ft) (1)	0.049434	0.049434	0.049434	0.049434	0.049434	0.049434	0.049434	0.049434	0.049434
LLDF Both Lanes (per ft) (1)	0.075988	0.075988	0.075988	0.075988	0.075988	0.075988	0.075988	0.075988	0.075988

FEA Computations

Span 1

PosTruckX (in)	42.000	42.000	42.000	156.00	156.00	156.00	216.00	216.00	216.00
loadcase	1.0000	2.0000	3.0000	1.0000	2.0000	3.0000	1.0000	2.0000	3.0000
group.One_Lane_Loaded	1.0000	0.0000	1.0000	1.0000	0.0000	1.0000	1.0000	0.0000	1.0000
group.Second_Lane_Loaded	0.0000	1.0000	1.0000	0.0000	1.0000	1.0000	0.0000	1.0000	1.0000
Length - Span 1 (ft)	40.000	40.000	40.000	40.000	40.000	40.000	40.000	40.000	40.000
FEA Width1 Net (in)	293.78	536.03	379.54	372.15	627.82	467.30	381.60	606.45	468.45
FEA Width2 Net (in)	190.52	218.95	203.75	232.05	232.07	232.06	231.74	217.65	224.47
FEA Ewidth1, in - Span 1 (in)	266.06	485.47	343.74	337.04	568.59	423.21	345.60	549.24	424.26
FEA Ewidth2, in - Span 1 Two lanes (in)	172.54	198.30	184.53	210.16	210.17	210.17	209.88	197.12	203.30
Skew Correction Factor	0.90566	0.90566	0.90566	0.90566	0.90566	0.90566	0.90566	0.90566	0.90566
Percent to Slab - Span 1 (1)	1.0000	1.0000	1.0000	1.0000	1.0000	1.0000	1.0000	1.0000	1.0000
Percent to Beams - Span 1 (1)	-8.5122E-8	-1.4920E-7	-1.1716E-7	-7.7814E-8	-1.3269E-7	-1.0525E-7	-1.2832E-7	-2.1563E-7	-1.7198E-7
MxTotalAll (Deck+Rails) - Span 1 (in*lbf)	3.8084E6	3.8084E6	7.6167E6	3.8087E6	3.8083E6	7.6170E6	3.8075E6	3.8081E6	7.6156E6
Mx Rail Left - Span 1 (in*lbf)	-0.012125	-0.019050	-0.031175	-0.0022877	-0.0072965	-0.0095842	-0.0010109	-0.010452	-0.011462
Mxx Deck - Span 1 (in*lbf)	3.8084E6	3.8084E6	7.6167E6	3.8087E6	3.8083E6	7.6170E6	3.8075E6	3.8082E6	7.6156E6
Mx Rail Right - Span 1 (in*lbf)	-0.31205	-0.54916	-0.86122	-0.29408	-0.49802	-0.79210	-0.48756	-0.81070	-1.2983
Average Mxx under one lane - Span 1 (lbf)	14314	7844.8	22159	11300	6697.8	17998	11017	6933.5	17950
Average Mxx under both lanes - Span 1 (lbf)	11036	9602.8	20639	9061.5	9059.9	18121	9070.8	9659.5	18730
LLDF One Lane Net - Span 1 (per ft) (1)	0.040847	0.022387	0.031617	0.032245	0.019114	0.025680	0.031446	0.019787	0.025616
LLDF Both Lanes Net - Span 1 (per ft) (1)	0.062987	0.054807	0.058897	0.051714	0.051709	0.051711	0.051783	0.055134	0.053458

For skewed bridges, the longitudinal force effects may be reduced by the factor, r:

$$r = 1.05 - 0.25\tan\theta \le 1.00 \qquad (4.6.2.3\text{-}3)$$

where:

θ = skew angle (degrees)

r = 1.05 – 0.25(tan 30)
r = 1.05 – 0.25(.577)
r = 0.906

E1 without skew = 0.0655
E1 with skew = 0.059

E1 without skew = 0.045
E1 with skew = 0.041

Figure 4.10 Skew factor output

4.8 Barrier Stiffness Effects

The final parametric study incorporated barrier rail stiffness. The barriers were modeled as 12 × 24 in. sections with stiffness properties A_x = 288 in², I_{zz} = 13,800 in⁴, I_{yy} = 3,456 in⁴, and J_x = 13,800 in⁴ made of concrete (see Figure 4.11).

Figure 4.11 Barrier stiffness data

Figure 4.12 provides effective widths and LLDFs, accounting for barrier stiffness.

Under edge loading, the loaded-side barrier (left) resisted approximately 41% of the total section moment; 53% was resisted by the deck, and only 6% by the opposite barrier (right). This distribution significantly increased the effective width from 266 to 456 in., reducing the LLDF from 0.045 to 0.026. Note, that M_x is the bending moment in the beam element with typical units

of ft-kip, where M_{xx} is the slab bending moment, which is moment per length with typical units of ft-kip/ft.

Detailed Computations (with barrier stiffness)

FEA Computations

Span 1

PosTruckX (in)	42.000	42.000	42.000	156.00	156.00	156.00	216.00	216.00	216.00
loadcase	1.0000	2.0000	3.0000	1.0000	2.0000	3.0000	1.0000	2.0000	3.0000
group.One_Lane_Loaded	1.0000	0.0000	1.0000	1.0000	0.0000	1.0000	1.0000	0.0000	1.0000
group.Second_Lane_Loaded	0.0000	1.0000	1.0000	0.0000	1.0000	1.0000	0.0000	1.0000	1.0000
Length - Span 1 (ft)	40.000	40.000	40.000	40.000	40.000	40.000	40.000	40.000	40.000
FEA Width1 Net (in)	455.94	851.61	593.96	425.32	808.21	557.33	422.07	822.85	557.95
FEA Width2 Net (in)	294.42	280.22	287.14	275.58	275.62	275.60	275.42	281.74	278.54
FEA Ewidth1, in - Span 1 (in)	241.90	559.33	352.63	278.16	528.55	364.49	282.16	500.10	356.05
FEA Ewidth2, in - Span 1 Two lanes (in)	156.21	184.05	170.47	180.23	180.25	180.24	184.12	171.23	177.75
Skew Correction Factor	1.0000	1.0000	1.0000	1.0000	1.0000	1.0000	1.0000	1.0000	1.0000
Percent to Slab - Span 1 (1)	0.53056	0.65679	0.59369	0.65401	0.65398	0.65400	0.66853	0.60776	0.63814
Percent to Beams - Span 1 (1)	0.46944	0.34321	0.40631	0.34599	0.34602	0.34600	0.33147	0.39224	0.36186
MxTotalAll (Deck+Rails) - Span 1 (in*lbf)	3.8049E6	3.8071E6	7.6120E6	3.8073E6	3.8070E6	7.6143E6	3.8063E6	3.8063E6	7.6126E6
Mx Rail Left - Span 1 (in*lbf)	1.5676E6	8.3681E5	2.4044E6	8.6312E5	4.5417E5	1.3173E6	6.3083E5	3.1746E5	9.4829E5
Mxx Deck - Span 1 (in*lbf)	2.0187E6	2.5005E6	4.5192E6	2.4900E6	2.4897E6	4.9797E6	2.5446E6	2.3133E6	4.8579E6
Mx Rail Right - Span 1 (in*lbf)	2.1856E5	4.6982E5	6.8838E5	4.5417E5	8.6312E5	1.3173E6	6.3083E5	1.1755E6	1.8064E6
Average Mxx under one lane - Span 1 (lbf)	8345.3	4470.5	12816	8951.7	4710.4	13662	9018.1	4625.7	13644
Average Mxx under both lanes - Span 1 (lbf)	6461.7	6793.0	13255	6907.8	6906.2	13814	6910.0	6754.9	13665
LLDF One Lane Net - Span 1 (per ft) (1)	0.026320	0.014091	0.020203	0.028214	0.014848	0.021531	0.028431	0.014583	0.021507
LLDF Both Lanes Net - Span 1 (per ft) (1)	0.040758	0.042823	0.041791	0.043544	0.043538	0.043541	0.043570	0.042592	0.043081

Computations:
Mx (total section) = 3808 in-kip
Skew factor = 1

Edge position:

a. Mx left rail = 1567 in-kip (41%)
b. Mx deck = 2019 (53%)
c. Mx right rail = 219 in-kip (6%)

M1xx (average) = 8.35 kip (FEA and include barrier effects)
E1 = 3808/8.35 = 456 in (266 in without barrier)
LLDF1 = 12 (in design section)/456 = 0.026

M2xx (average) = 13.3 kip (FEA and include barrier effects)
E2 = 3808/13.3 = 286 in (185 in without barrier)
LLDF1 = 12 (in design section)/286 = 0.042

Figure 4.12 Detailed LLDF computations considering edge barrier stiffness – edge loading position

Figure 4.13 illustrates the moment distribution with barriers included. Here, the barriers shared load symmetrically, each resisting 16.5% of the moment, with the deck carrying 67%. The effective width in this case was 422 in., compared to 346 in. without barriers, $E_{1AASHTO}$ = 220 in.

These results demonstrate the importance of barrier stiffness in slab bridge behavior. While AASHTO distribution factors do not explicitly consider barrier effects, the analysis suggests that stiff barriers can meaningfully reduce slab demand and may justify higher rating factors. This observation is consistent with the literature discussed in Chapter 1.

Detailed Computations (with barrier stiffness)

FEA Computations

Span 1

PosTruckX (in)	42.000	42.000	42.000	156.00	156.00	156.00	216.00	216.00	216.00
loadcase	1.0000	2.0000	3.0000	1.0000	2.0000	3.0000	1.0000	2.0000	3.0000
group.One_Lane_Loaded	1.0000	0.0000	1.0000	1.0000	0.0000	1.0000	1.0000	0.0000	1.0000
group.Second_Lane_Loaded	0.0000	1.0000	1.0000	0.0000	1.0000	1.0000	0.0000	1.0000	1.0000
Length - Span 1 (ft)	40.000	40.000	40.000	40.000	40.000	40.000	40.000	40.000	40.000
FEA Width1 Net (in)	455.94	851.61	593.96	425.32	808.21	557.33	422.07	822.85	557.95
FEA Width2 Net (in)	294.42	280.22	287.14	275.58	275.62	275.60	275.42	281.74	278.54
FEA Ewidth1, in - Span 1 (in)	241.90	559.33	352.63	278.16	528.55	364.49	282.16	500.10	356.05
FEA Ewidth2, in - Span 1 Two lanes (in)	156.21	184.05	170.47	180.23	180.25	180.24	184.12	171.23	177.75
Skew Correction Factor	1.0000	1.0000	1.0000	1.0000	1.0000	1.0000	1.0000	1.0000	1.0000
Percent to Slab - Span 1 (1)	0.53056	0.65679	0.59369	0.65401	0.65398	0.65400	0.66853	0.60776	0.63814
Percent to Beams - Span 1 (1)	0.46944	0.34321	0.40631	0.34599	0.34602	0.34600	0.33147	0.39224	0.36186
MxTotalAll (Deck+Rails) - Span 1 (in*lbf)	3.8049E6	3.8071E6	7.6120E6	3.8073E6	3.8070E6	7.6143E6	3.8063E6	3.8063E6	7.6126E6
Mx Rail Left - Span 1 (in*lbf)	1.5676E6	8.3681E5	2.4044E6	8.6312E5	4.5417E5	1.3173E6	6.3083E5	3.1746E5	9.4829E5
Mxx Deck - Span 1 (in*lbf)	2.0187E6	2.5005E6	4.5192E6	2.4900E6	2.4897E6	4.9797E6	2.5446E6	2.3133E6	4.8579E6
Mx Rail Right - Span 1 (in*lbf)	2.1856E5	4.6982E5	6.8838E5	4.5417E5	8.6312E5	1.3173E6	6.3083E5	1.1755E6	1.8064E6
Average Mxx under one lane - Span 1 (lbf)	8345.3	4470.5	12816	8951.7	4710.4	13662	9018.1	4625.7	13644
Average Mxx under both lanes - Span 1 (lbf)	6461.7	6793.0	13255	6907.8	6906.2	13814	6910.0	6754.9	13665
LLDF One Lane Net - Span 1 (per ft) (1)	0.026320	0.014091	0.020203	0.028214	0.014848	0.021531	0.028431	0.014583	0.021507
LLDF Both Lanes Net - Span 1 (per ft) (1)	0.040758	0.042823	0.041791	0.043544	0.043538	0.043541	0.043570	0.042592	0.043081

Computations:
Mx (total section) = 3808 in-kip
Skew factor = 1

Middle one lane position (#3):

a. Mx left rail = 631 in-kip (16.5%)
b. Mx deck = 2544 (67%)
c. Mx right rail = 631 in-kip (16.5%)

M1xx (average) = 9.02 kip (FEA and include barrier effects)
E1 = 3808/9.02 = 422 in (346 in without barrier)
LLDF1 = 12 (in design section)/422 = 0.028

Figure 4.13 Detailed LLDF computations considering edge stiffness - middle loading position

4.9 Non-standard Axle Gages

The base example is extended to include the use case for a permit vehicle with non-standard axle spacing. Figure 4.14 illustrates a truck with 40-kip wheel loads with four wheels on the trailer, spaced at 5-, 10-, and 5-ft. For large (super) loads, wider axles are commonly used to spread the load. This axle distributes the load effects similar to a two-lane case; moreover, the truck is often required to run in the middle of the bridge. Note that the actual bending moments are determined from a beamline analysis, e.g., BrR, using the axle loads and longitudinal spacings.

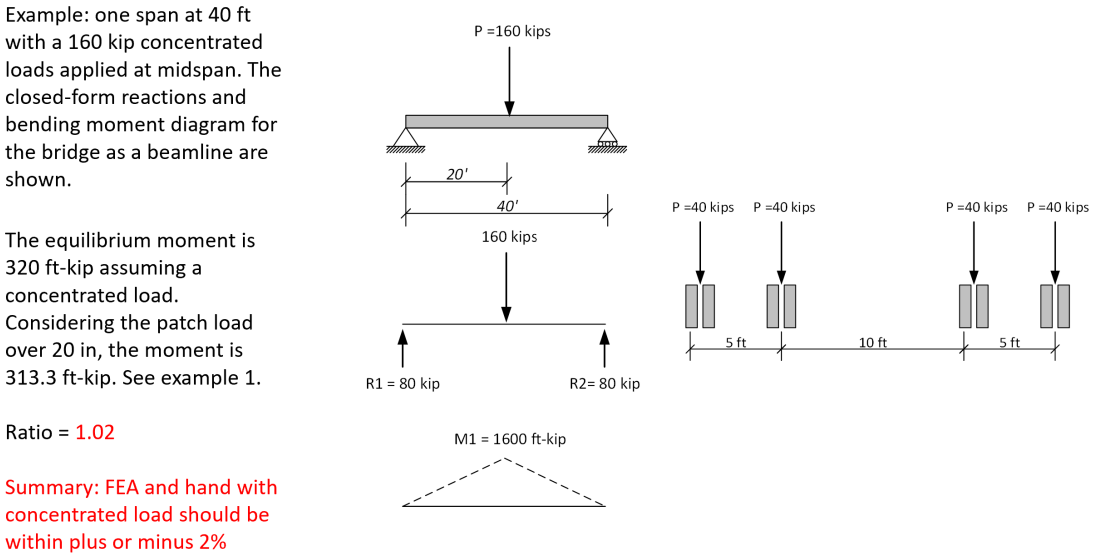

Figure 4.14 Permit a truck with non-standard axle spacing

The load for the non-standard gage is defined similarly to the two-lane situation. However, as illustrated later in this extension, the interpretation of results changes. Figure 4.15 provides the truck definition, and other values are the same for the bridge.

The left side of the truck uses the first lane position, and the right side uses the second lane position. The two-lane effective width and LLDF are used; however, because this model has one truck, the effective width is double, or the LLDF is decreased by 50%.

Figure 4.16 illustrates the load position and meshing. Figure 4.17 shows the bending moments and analysis section for computing the average moment. Figure 4.18 plots the bending moment across the midspan section, and Figure 4.19 uses this plot to demonstrate effective width and LLDF computations. Note that this analysis does not include the barrier stiffness effects; the inclusion of this stiffness would further decrease the load effects. The effect of barrier stiffness will be more pronounced for an edge-load position, i.e., no restriction on the travel path for the permit.

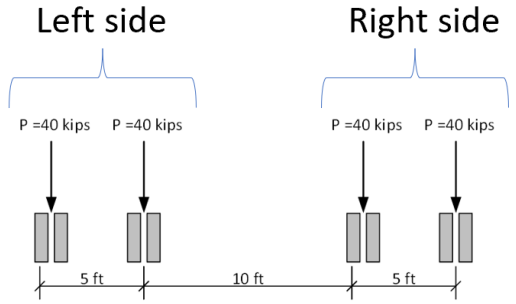

For permits:

- Use the “primary” as the left side
- Use the “secondary” as the right
- Use the both lanes load results
- Double the effective widths because N_{lane} is 1.0

Figure 4.15 Load definition for non-standard axle example

Mesh

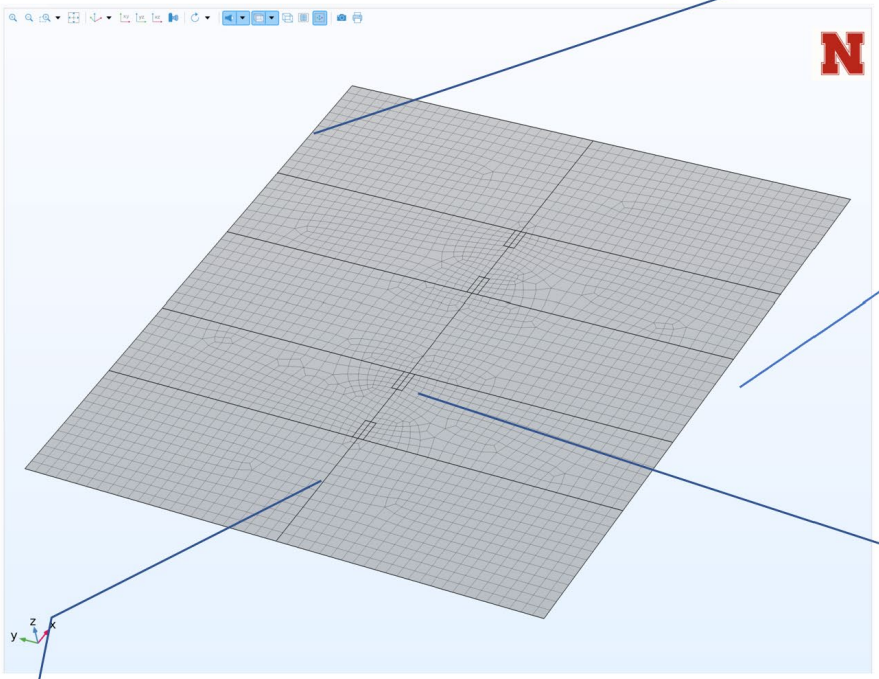

Simple Supports

Wheel Patch Loads = 40 kips (uniform load)
Use both lanes loaded computations

Evaluation Section $M_{equilibrium}$ = 160 kips (40 ft)/4 = 1600 ft-kip = 19200 in-kip (also beamline for design)

Figure 4.16 Load Position and Meshing

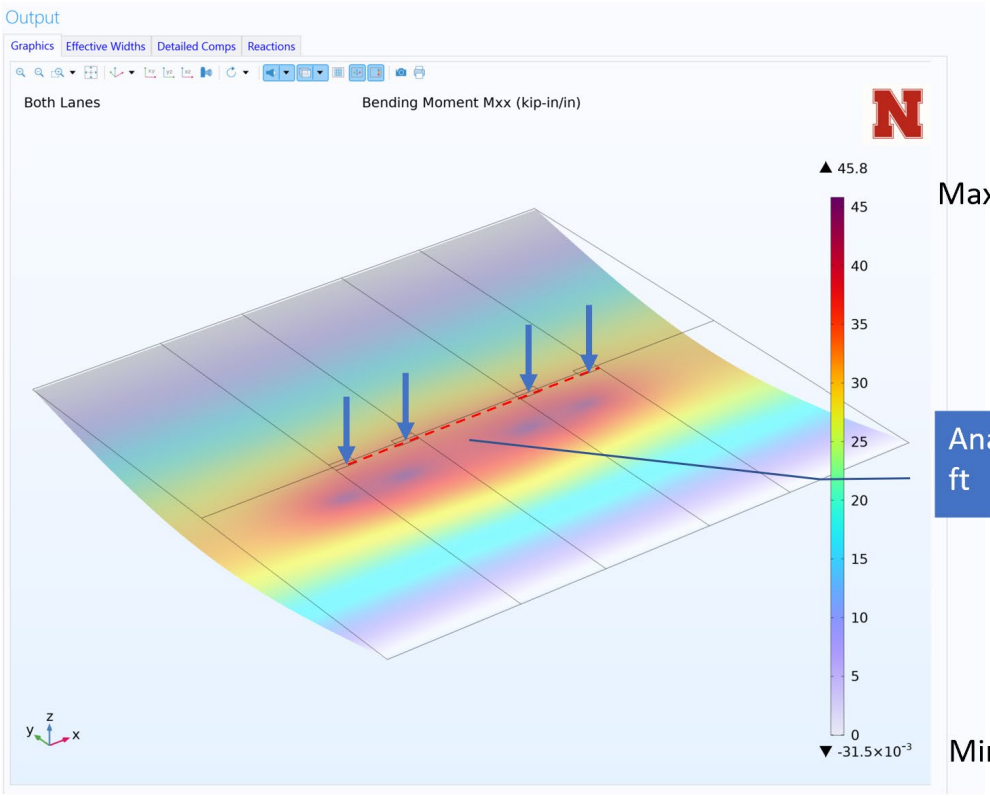

Max M_{xx} = 48.5 kips

Analysis section = 2(60 + 20) +120 = 280 in = 23.33 ft

Min M_{xx} = 0.0 kips

Figure 4.17 Load position and bending moments

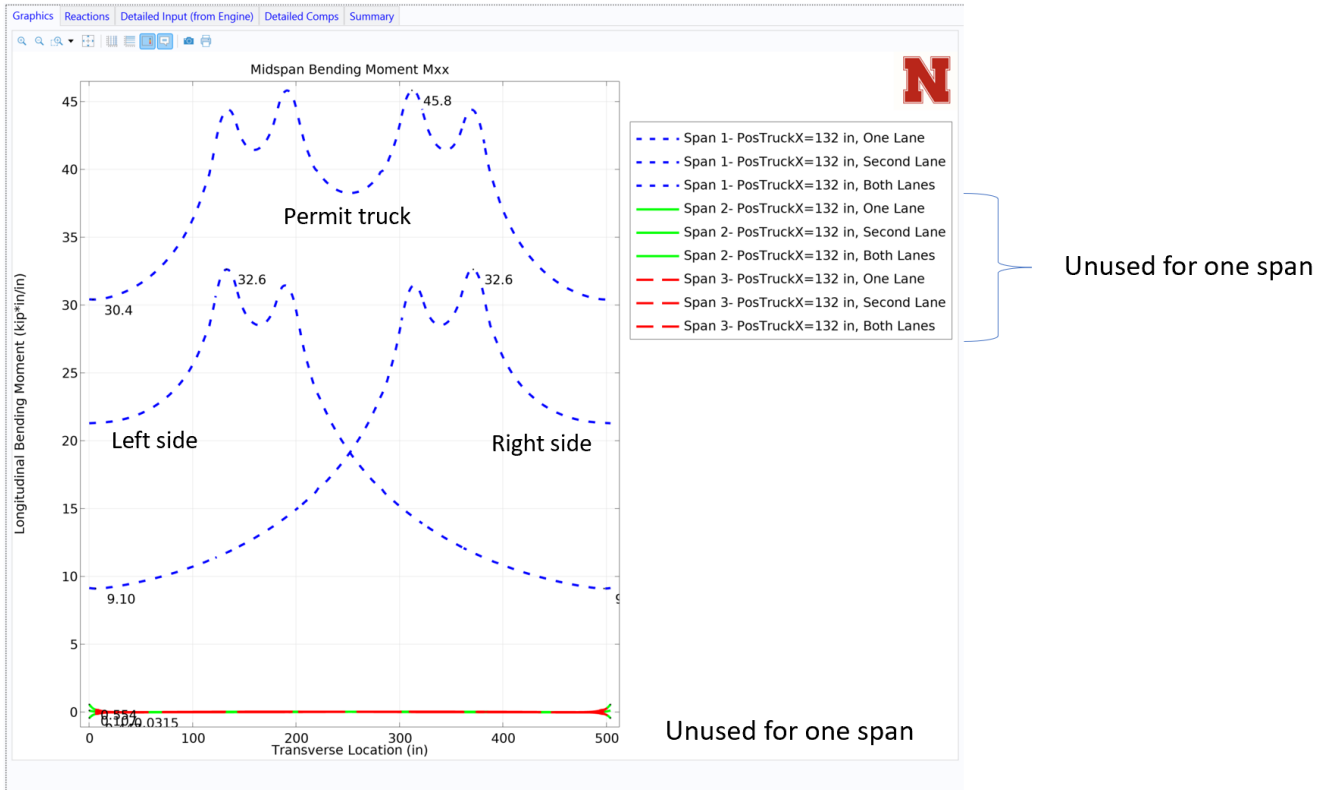

Figure 4.18 Transverse plot of bending moments

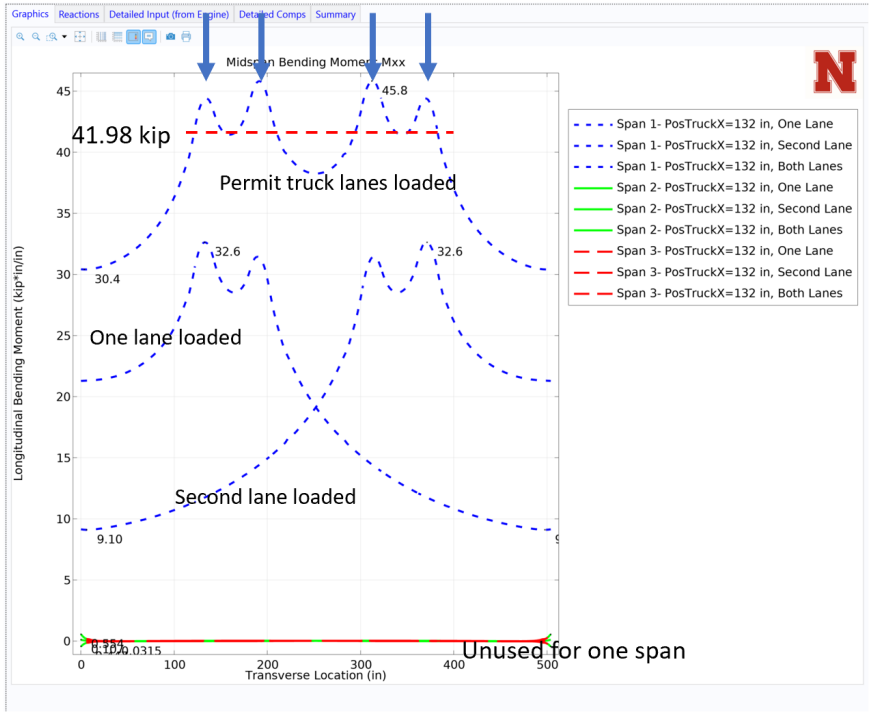

$M_{total-permit}$ (from statics) = 1600 ft-kip = 19200 in-kips
$M_{total-permit}$ (from FEA) = 19040 in-kips
$M_{Average\ between\ axles-one\ lane}$ = 41.97 kips

E_{permit} = 19040/41.98 = 454 in = 37.8 ft
$LLDF_{permit}$ = 12/454 = 0.026

Using the max M_{xx} = 45.8 kip
E_{permit} = 1600/45.8 = 35 ft = 420 in
$LLDF_{permit}$ = 12/420 = 0.029

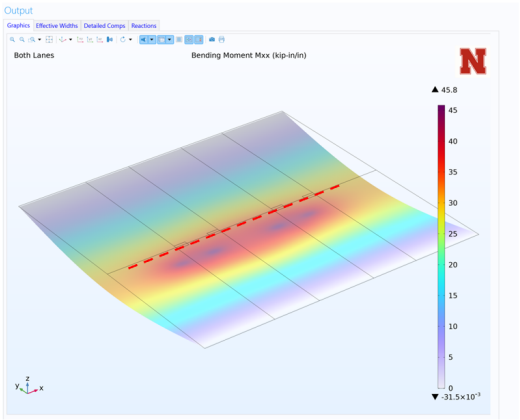

Bridge width = 42 ft, most of the bridge is used

Figure 4.19 Computations for the effective width and LLDF

4.10 Culminating Example

AASHTO MBE Example A7 was used to illustrate effective width computations in a comprehensive example that compares different options for position and barrier rail stiffness. See Figure 20 for the cross section, the bridge has one span of length 20.5 ft.

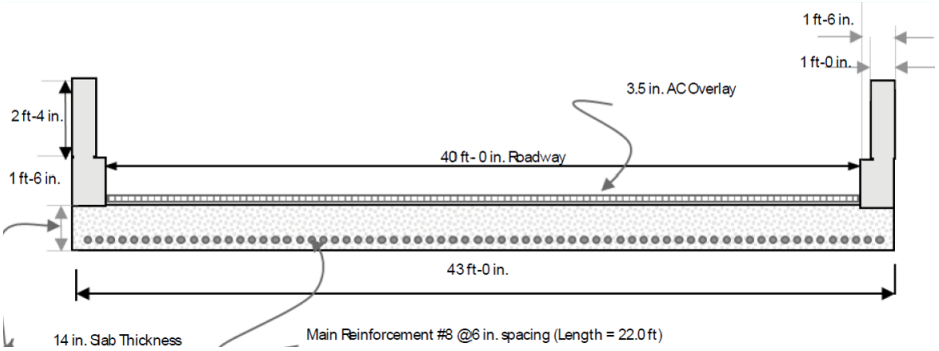

Figure 20. AASHTO MBE Example A7 Cross Section

Table 2 provides the effective width for the AASHTO equations and the edge strip width for one wheel line, which is doubled here to account for a full lane. Column 3 provides the FEA solution. Using the equations for E1 (without multiple presence) and E2, the increase in effective width is about 25%; using the edge strip rules, the increase is 52%. For load placement in the middle of the deck, which is more of a rating use case, the increases are 63% and 41% for one- and two-lane loads. This clearly demonstrates the benefits of considering load positioning.

Table 3 presents results for the edge-stiffened case and is structured similar in Table 2. As expected, the barrier significantly affects edge loading, with 73 to 81 percent of the load carried by the slab (27 to 19 percent by the barrier rail), resulting in an effective width increase of 46 to 100 percent at the edge load position. In the middle of the bridge, the load on the barrier rail decreases, as the rail has little effect on the interior, especially for a short span, as in this example.

Table 2. AASHTO MBE Example A7 (not considering barriers, Effective widths, in.

No. Lanes Loaded	Load Position	FEA	AASHTO E1 (m = 1.2)	AASHTO E2 (m = 1.0)	Ratio
1	Edge	207	137	164	207/164 = 1.26
2	Edge	158	n/a	128	159/128 = 1.24
1	Edge strip rules	207	136	136	207/136 = 1.52
2	Edge strip rules	158	136	136	n/a
1	Middle	267	183	164	267/183 = 1.63
2	Middle	180	n/a	128	180/128 = 1.41

Table 3. AASHTO MBE Example A7 (considering rail stiffness), Effective width, in.

No. Lanes Loaded	Load Position	FEA/ Model	Percent to Slab	AASHTO E1 (m = 1.2)	AASHTO E2 (m = 1.0)	Ratio
1	Edge	274	73	137	164	274/164 = 1.67
2	Edge	187	81	n/a	128	187/128 = 1.46
1	Edge strip rules	274	73	136	136	274/136 = 2.01
2	Edge strip rules	187	n/a	136	136	187/136 = 1.14
1	Middle	261 277	92	183	n/a	267/164 = 1.64 277/183 = 1.51
2	Middle	182 204	90	n/a	128	182/128 = 1.42 204/128 = 1.59

Extending this example to two spans yields similar results; however, due to space constraints, those results are not presented.

4.11 Implications and Discussion

This validation study provides several practical insights:

- Reliability of FEA: The excellent agreement between statics and finite element solutions confirms the modeling approach.
- Code alignment: FEA-derived LLDF values are lower than the AASHTO equations, but within reasonable ranges, for edge loads.
- Enhanced insight: FEA captures the transverse slab stiffness and optionally the barrier stiffness, which can either amplify or relieve demands. In practice, this means that conservative assumptions in simplified equations may be relaxed when advanced modeling demonstrates beneficial stiffness contributions.
- Practice: Culminating Example demonstrates practical application and range of potential benefits from refined modeling.
- Bridge management relevance: These results show where the payoff occurs for agencies considering whether to invest in rigorous modeling.

4.12 Summary

In summary, the one-span slab bridge example demonstrates that finite element modeling is both accurate and informative. The key outcomes are:

- Midspan moments from statics and FEA within ±2%. This is an important validation check.
- SAP 2000 models compared well with SlabDF. This helps to validate the overall stiffness model.
- FEA-based LLDFs for edge loading are about 20% less than the AASHTO equations. This is expected given the development of the equation.
- Load position plays a large role in the LLDF, with loads located in the middle having lower LLDFs.
- Barrier stiffness substantially increased effective widths and lowered LLDFs, highlighting their structural role.

Overall, the study demonstrates significant benefits through rigorous analysis that considers load position and/or barrier rail stiffness.

Chapter 5 Additional Examples

The appendices present several examples as PowerPoint presentations, including the example provided in Chapter 4, where the most important figures and narratives provide detailed explanations for this example. Narratives for all examples were not provided as the text would be highly redundant and monotonous.

Table 5.1 Summary of Examples

Example	Appendix	Comments
One-span	A	Chapter 4 provides a narrative that highlights and explains the use and interpretation of the results. It also provides methods for checking the analysis.
Two-span	B	This uses two 40-ft spans. It illustrates the symmetry where expected, negative moments near the support, use of the continuous beamline tool for equilibrium moments and reactions, and finally, it compares FEA to AASHTO results.
Three-span	C	This repeats the two-span example with 30-40-20 ft spans.
Three-span SAP 2000™ comparison	D	28-40-24 ft spans are modeled with SlabDF compared to a similar analysis performed in SAP 2000. The results are very similar. This checks the fundamental COMSOL formulation and usage with an independent program.

Chapter 6 Rail Stiffness Study

6.1 Introduction

During NDOT reviews and discussions, the issue of rail stiffness arose. For example, it is fairly apparent that a solid concrete barrier would provide composite action and likely the strength necessary to withstand a significant load from the deck. However, it is less apparent if a concrete barrier is composed of posts at regular spacing (see Figure 6.1).

To help provide guidance, a brief informal study was conducted. This study was beyond the scope of the proposed work but hopefully will provide insights or suggestions regarding future research.

6.2 Analysis

The rail geometry is typical of NDOT concrete rails. The model was developed parametrically (see Figure 6.2). A parametric sweep can change any parameter. In this case, the length of the post was studied. The post lengths were 3, 6, 12, 18, 24, 30, and 36 inches. The bridge is uniformly loaded with 100 psf and has pin-roller supports. The elements are concrete and solid, E = 3600 ksi. The meshing plots are provided in Figure 6.3 and Figure 6.4.

A typical normal stress plot is shown in Figure 6.5. Note the hotspot local stresses in the end posts. This is due to the large shear forces required near the end of the structure. Figure 6.6 and Figure 6.7 show normal stresses. Note that a shear force in the post bends the post, creating normal stresses. These small values were used to see the lower-bound behavior, even though they may be unrealistic.

Around 12 inches, the rail begins to work compositely. Figure 6.8 demonstrates the increase in compressive stress on the top of the rail, i.e., it is acting compositely with the deck. After 18 inches, there is little increase in compressive stress, i.e., it is nearly fully composite. Figure 6.9, Figure 6.10, Figure 6.11, and Figure 6.12 show the larger rail sizes.

6.3 Summary

As is typical of relative stiffness behavior, once a component becomes “stiff”, further stiffening will have little effect on load distribution. This is illustrated in Figure 6.13 where, after 12 inches, there is little increase in stress in the rail.

This study shows that a large concrete post is not needed to join the rail and the deck compositely. SlabDF assumes composite action, so this study should provide insight into that assumption. If desired, a small application could be developed for the rail as part of a future effort.

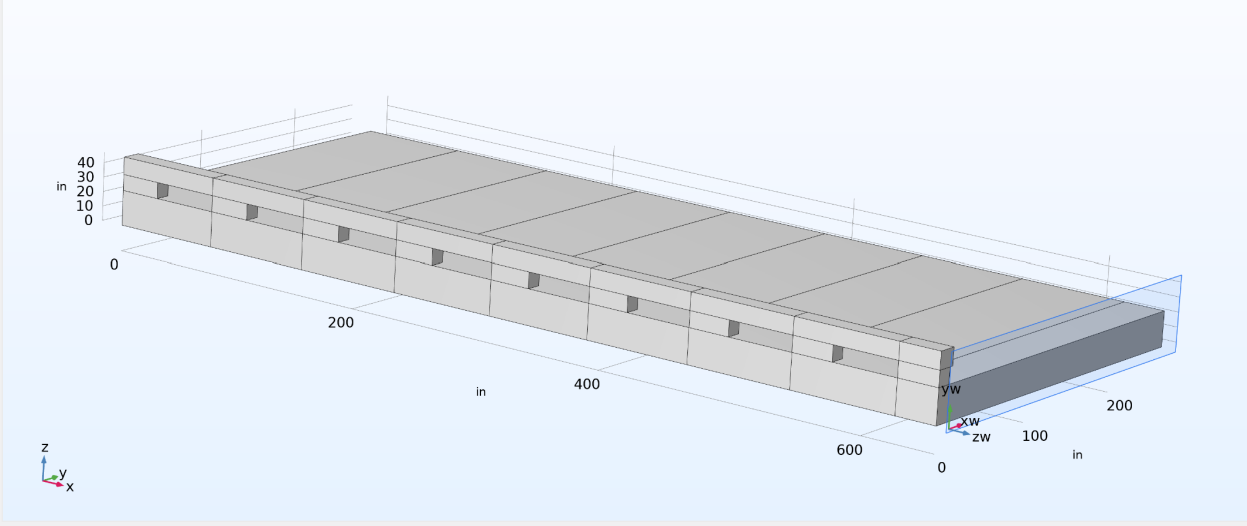

Figure 6.1 Parametric Rail Model

Label: Parameters 1

Parameters

Name	Expression	Value	Description
Brail	14[in]	14 in	Rail width
Hrail	12[in]	12 in	Rail height
Bpost	11[in]	11 in	Post width
Hpost	11[in]	11 in	Post height
Lpost	30[in]	30 in	Post length
Spost	6.5[ft]	78 in	Post spacing
Tdeck	24[in]	24 in	Deck thickness
Wdeck	44[ft]	528 in	Deck width
Nseg	9	9	Number of rail segments
Load	100 [lbf/ft^3]	0.05787 GIPS...	Uniform load on deck psf
L	Spost*2*(Nseg)-Spost	1326 in	Bridge length

Figure 6.2 Parametric Baseline Data

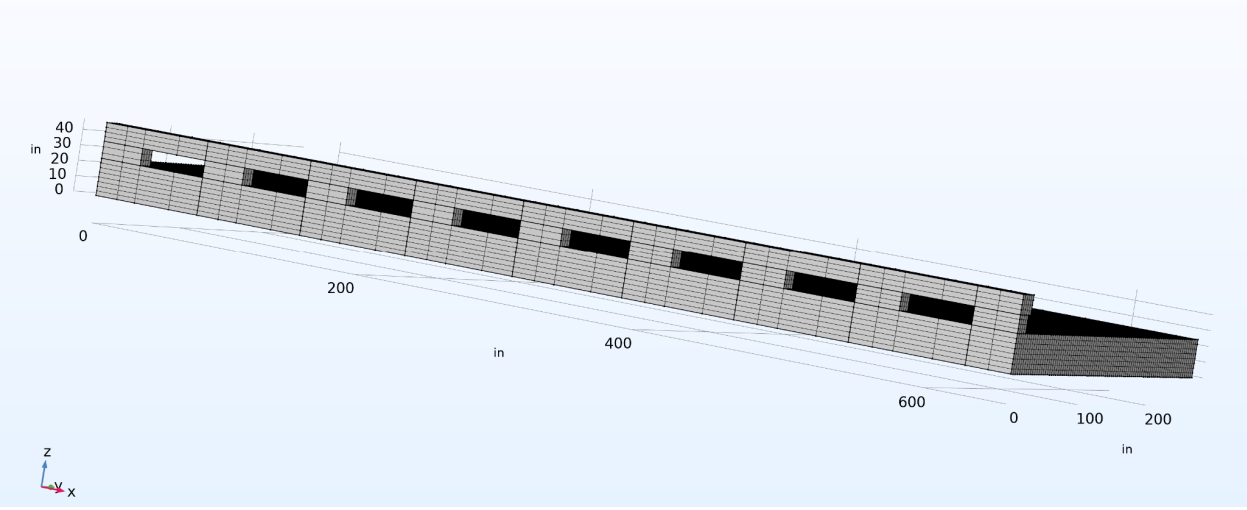

Figure 6.3 Meshing Elevation View

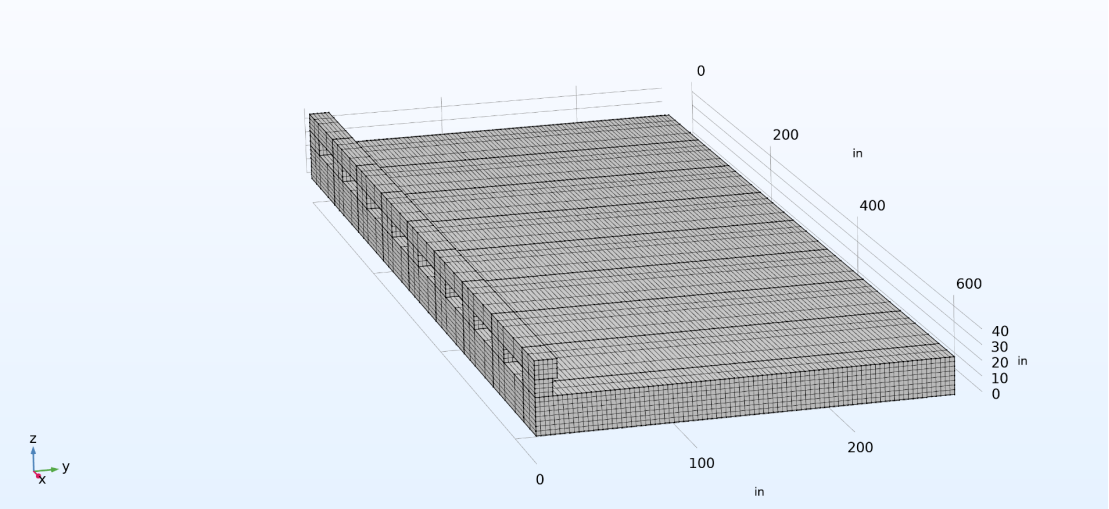

Figure 6.4 Meshing Cross-Section View

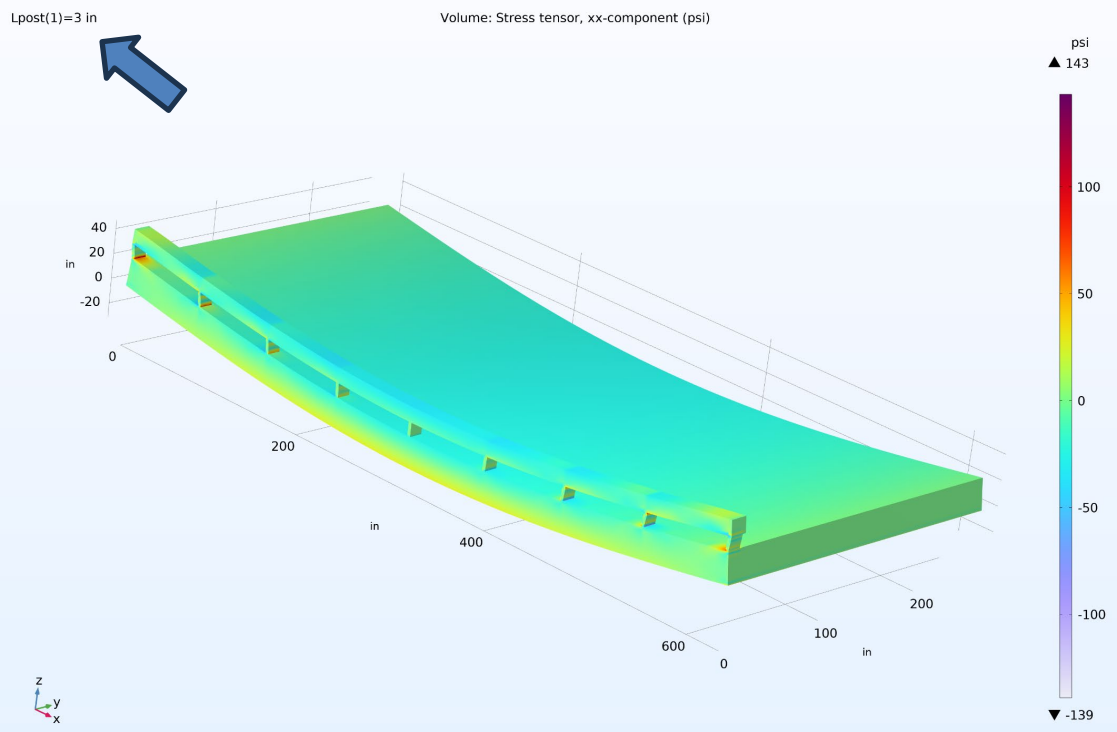

Figure 6.5 Normal Stress in the Longitudinal Direction (3-in post)

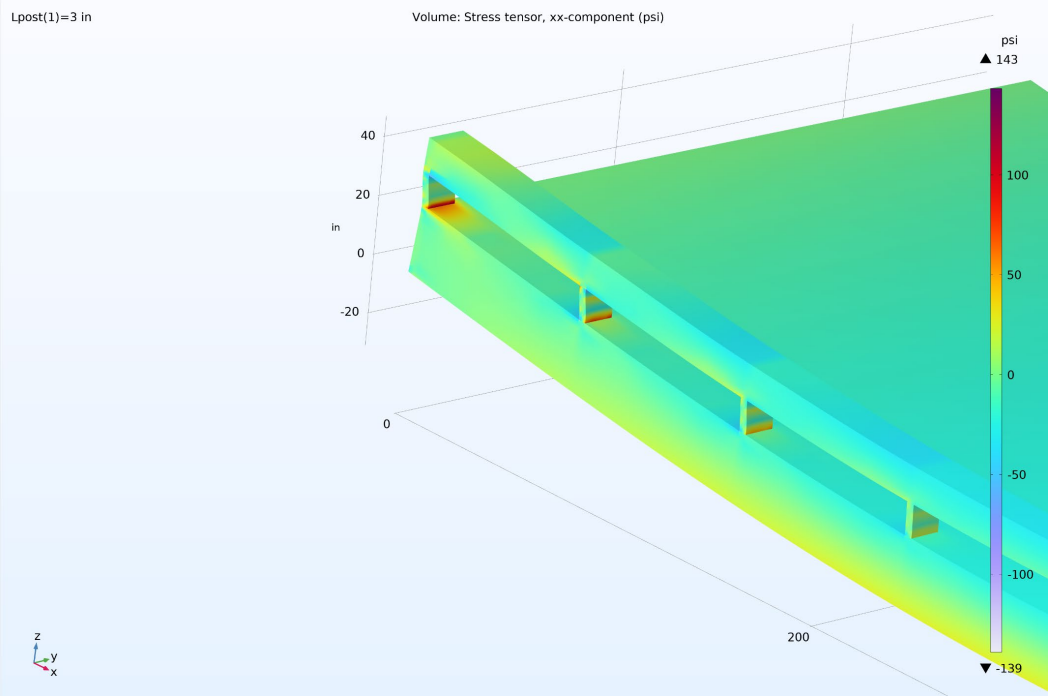

Figure 6.6 Local Post Stresses (3-in post)

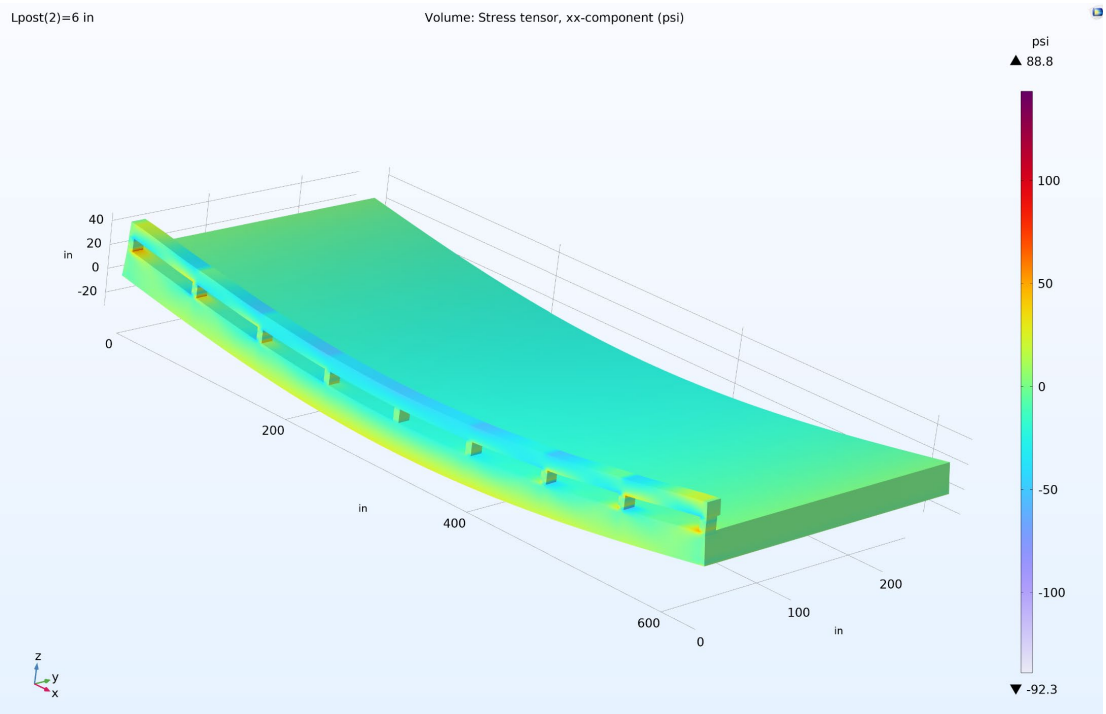

Figure 6.7 Local Post Stresses (6-in post)

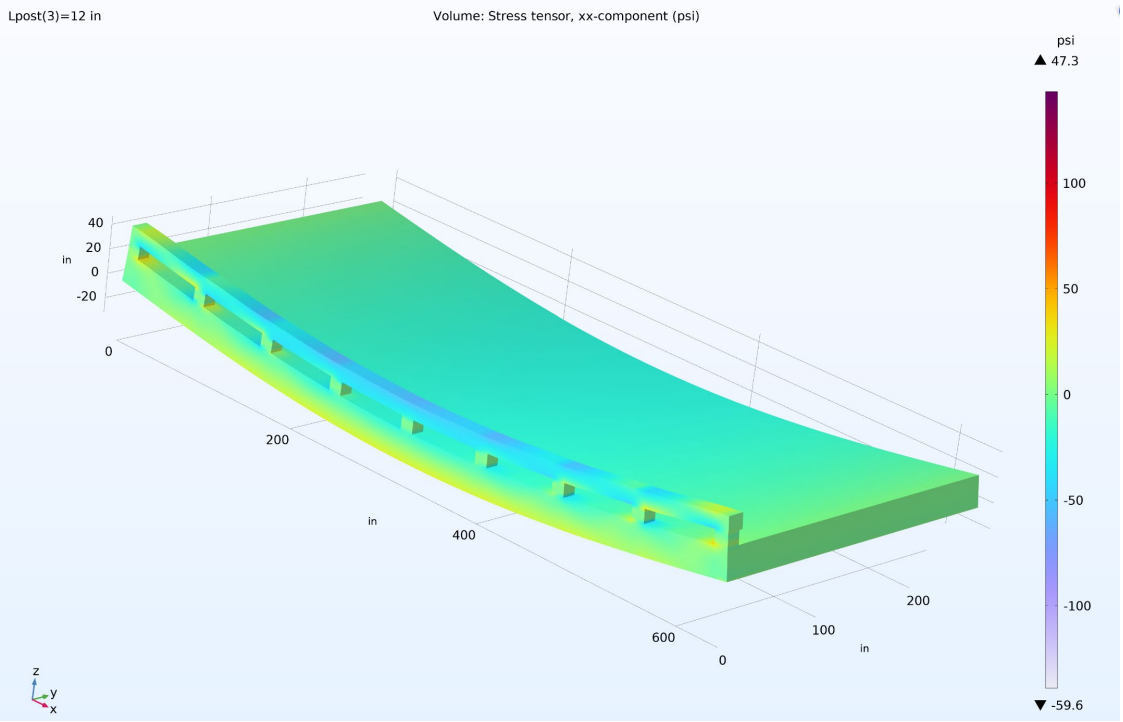

Figure 6.8 Normal Stress in the Longitudinal Direction (12-in post)

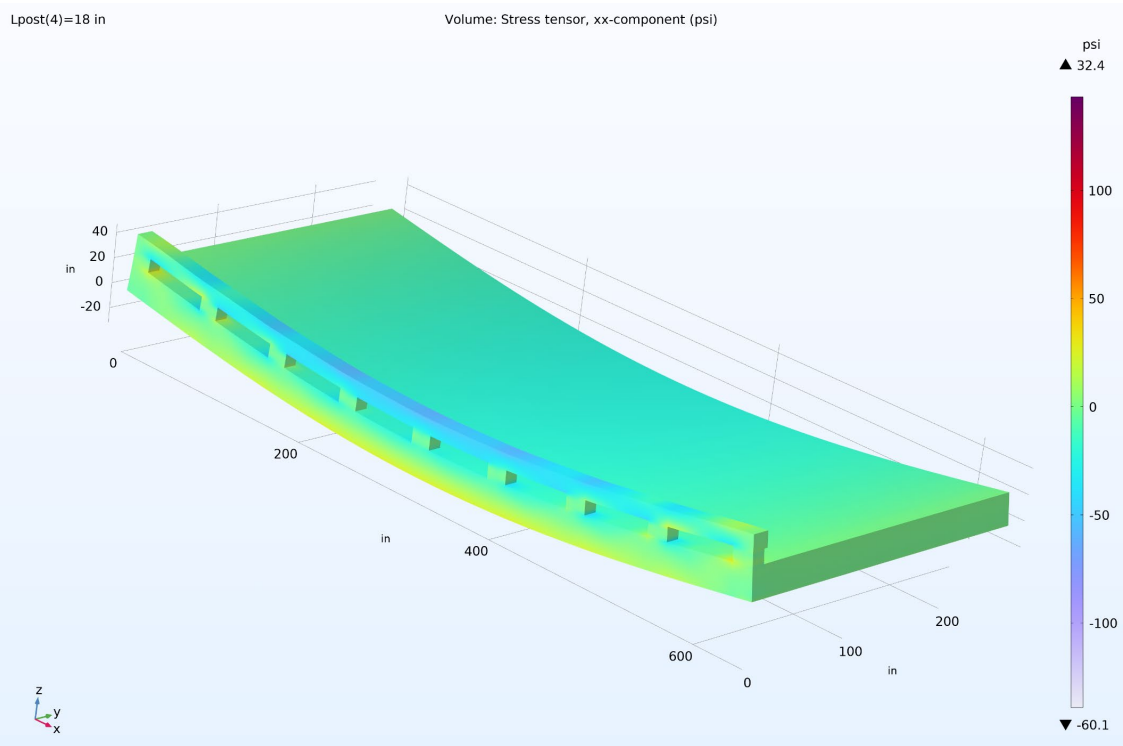

Figure 6.9 Normal Stress in the Longitudinal Direction (18-in post)

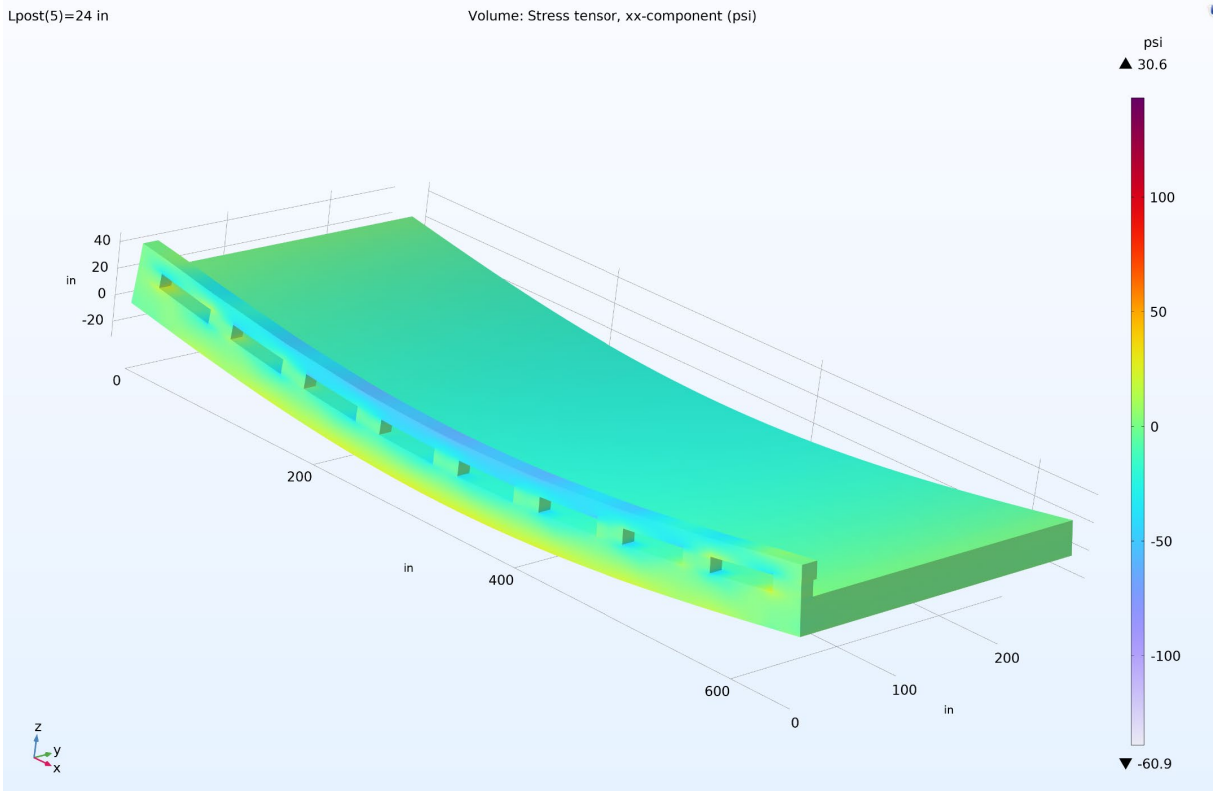

Figure 6.10 Normal Stress in the Longitudinal Direction (24-in post)

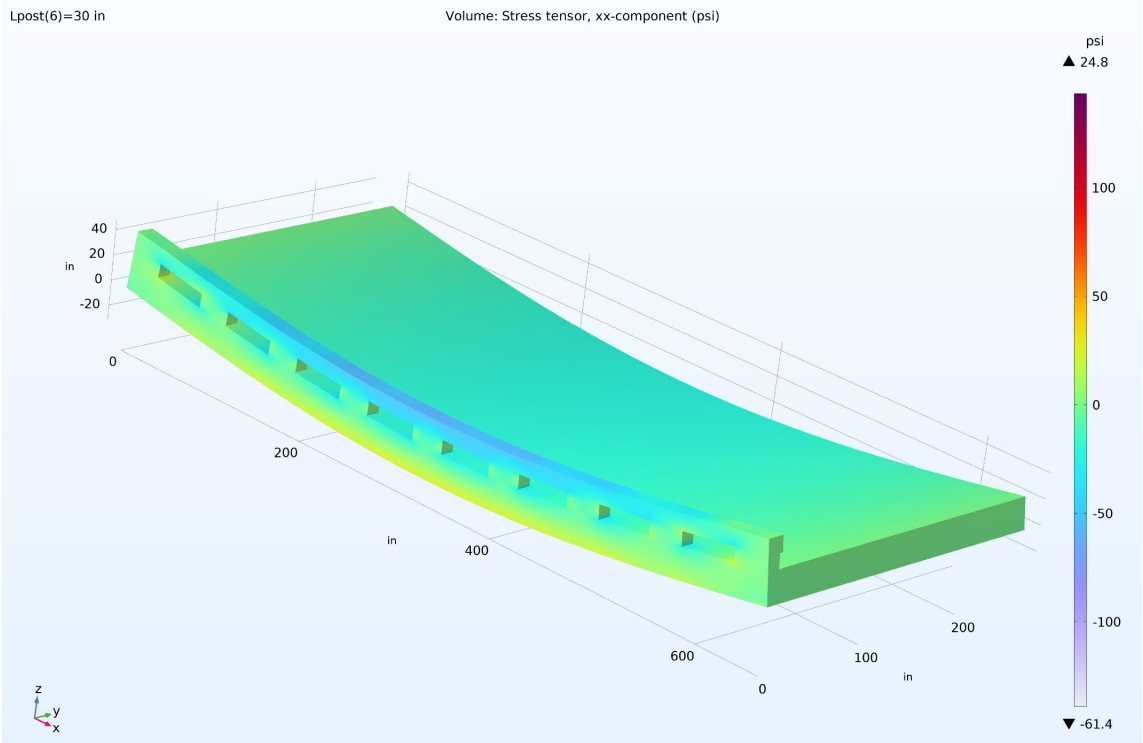

Figure 6.11 Normal Stress in the Longitudinal Direction (30-in post)

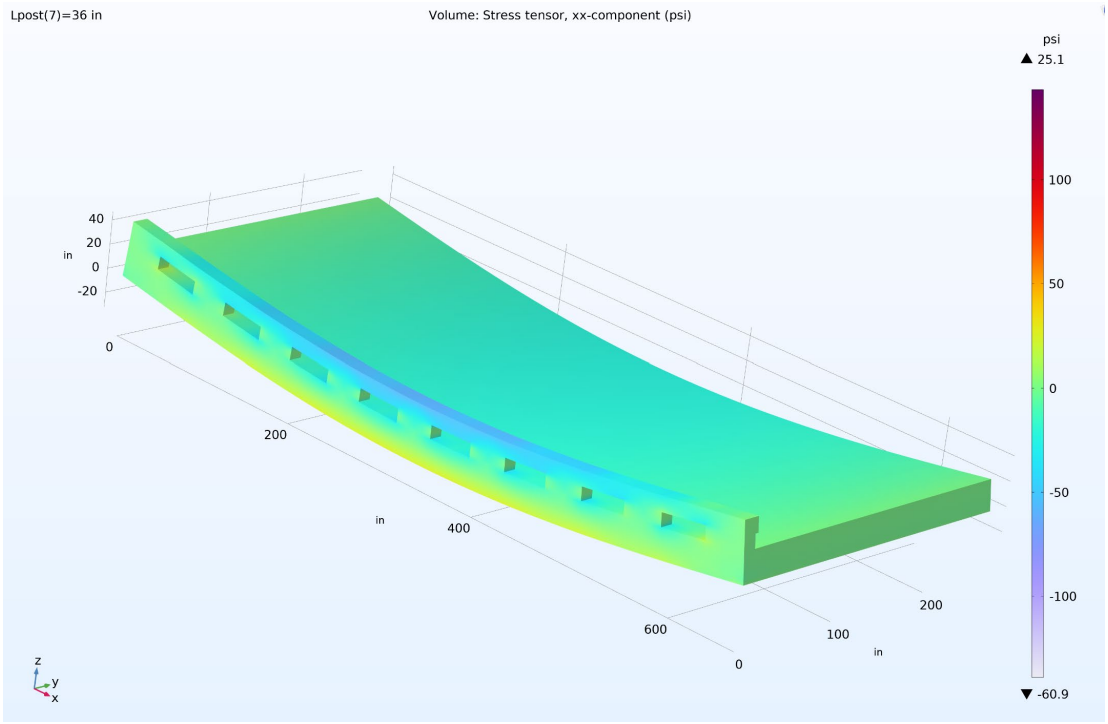

Figure 6.12 Normal Stress in the Longitudinal Direction (36-in post)

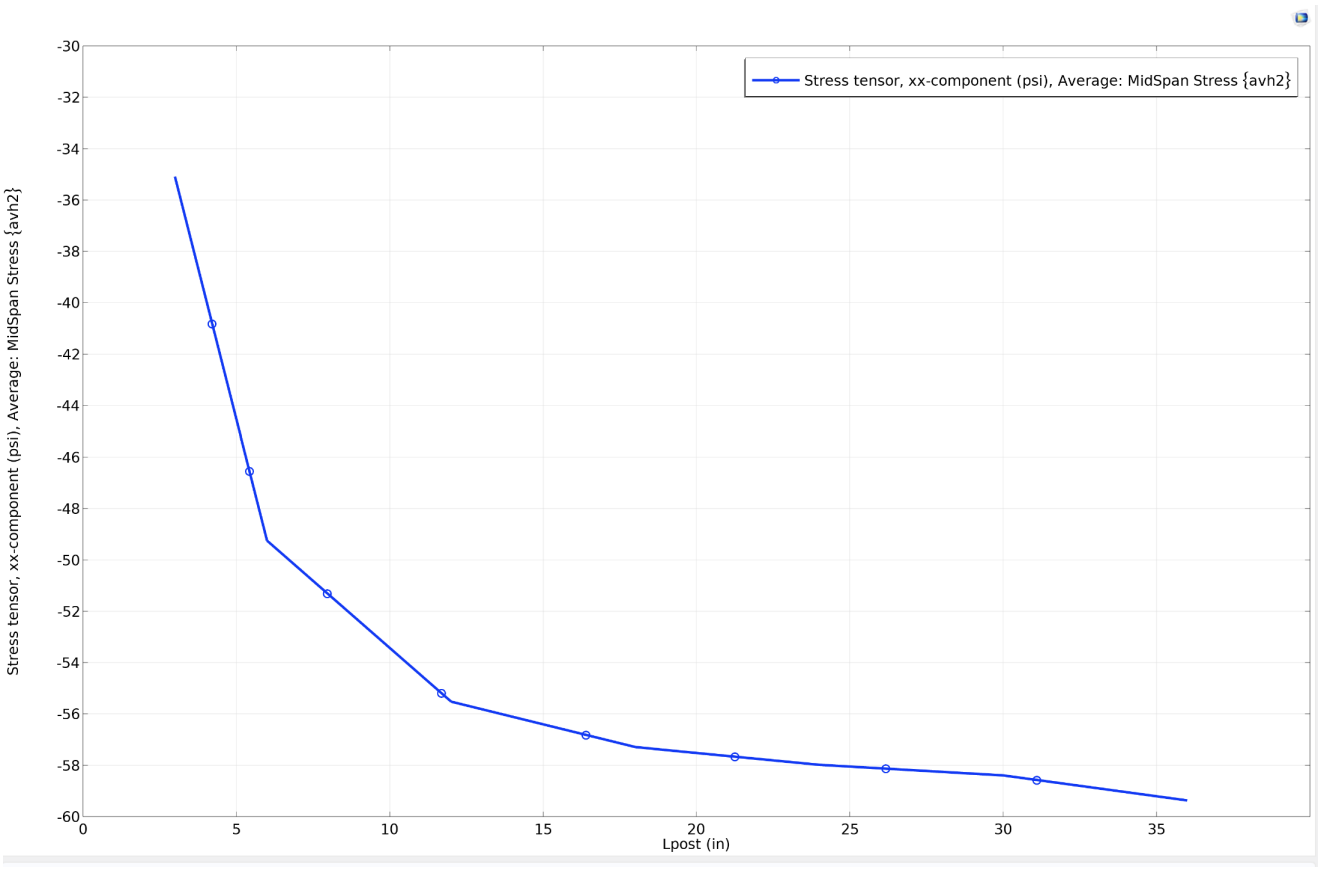

Figure 6.13 Compressive Stress in the Longitudinal Direction at the Top of the Rail

Chapter 7 NDOT Implementation

It is envisioned that NDOT engineers will run the application, compute effective widths, and enter results into BrR as part of their workflow. A spreadsheet was developed to illustrate how to import the SlabDF results into a spreadsheet and position the data in a manner similar to what is required in BrR.

This spreadsheet was developed in close collaboration with NDOT engineers. NDOT provided the first draft, which the research team iterated on to produce the next version. NDOT will maintain this sheet(s) to align with policies and procedures. Other owners or consultants can tailor a spreadsheet to meet specific requirements. See Table 7.1 for the path through the Excel spreadsheet.

Table 7.1 BrR and SlabDF Data Interface

Description	Figure
Instruction and truck positions	Figure 7.1
Bridge Geometry and analysis strip width, establish either exterior or interior beamline, define inflection points for BrR	Figure 7.2
Paste in the table from SlabDF	Figure 7.3
A summary of distribution factors is derived from Figure 7.3	Figure 7.4
Information required for BrR is derived from Figure 7.4	Figure 7.5
Input for BrR is shown with the data from Figure 7.5	Figure 7.6
Beamline analysis for inflection points	Figure 7.7

The data entry cells are light yellow. The green cells contain pasted information from SlabDF, the white cells contain computed data, and the red cells contain comments that might be removed in the future.

NEBRASKA
Good Life. Great Journey.
DEPARTMENT OF TRANSPORTATION
BRIDGE DIVISION

CN:		Subject:			
Project No:					
Bridge No:		By:		Date:	

Goal:	The goal of this spreadsheet is to convert the results from the Slab DF for refined analysis of slab bridges to the input required by BrR. This tab is for LRFR. A see other tab for LFR.

Instructions:	Fill out the bridge geometry information, the inputs from BrR model information, and the outputs from Slab DF. Indicate which truck positions should be used in the results (with an "x"). This spreadsheet will provide the distribution factors in the same format as required by BrR. Copy over the DF to BrR and run model. Create as many tabs as required for each member, load case, etc. Save as copy of this spreadsheet as pdf in the load rating calculations. Add a note in BrR saying that the DF were determined based on refined analysis of the structure.

File Name:	C:\UNL\Research\NDOT slab\NDOT feedback 2025-06-30\[Mock up - slab load rating - Refined DF spreadsheet-V1-JP-2025-08-18.xlsx]Slab DF
Date from System:	9/22/2025

Administration:	
Password to unlock fixed cells:	NDOT
Version:	Proto 2
Last modifed date:	
Modified by:	
TBD	
TBD	

Wheel Positions for Slab DF

This section is to record the wheel positions used in Slab DF.

Required: Pos truck1 < Pos truck2 < Pos truck3.

Use Case:	*Routine*	Comment:	*A comment goes here*		
			Default	**User specified**	
	Typical uses		Truck Position (in)	Description	Truck Position Used, in
Truck Position 1	First wheel 2 ft from face of rail		*38*		
Truck Position 2	2 trucks in the middle of the bridge		*134*		
Truck Position 3	1 truck in the middle of the bridge		*194*		

Figure 7.1 Spreadsheet linking SlabDF and BrR

Bridge Geometry (from Slab DF)		
Span 1	*26.660*	ft
Span 2	*40.000*	ft
Span 3	*26.660*	ft
Total Length	93.3200	ft
Number of Spans	3	

Inputs are in this color
xx are in this color -- second color TBD
Inputs (paste from Slab DF are in this color

Note: span length could come automatically from SlabDF data?

Strip location	Strip Width	
Exterior	*60*	in
Interior	120	in

Figure 7.2 Spreadsheet linking SlabDF and BrR

Outputs from Slab DF		Values in this table from "From Slab DF" tab																		
Summary Table from Slab DF	Positions	Load Cases/Factors			Span 1			Support 2			Span 2			Support 3			Span 3		
[redacted]	PosTruckX (in)	loadcase	group.One_Lane_Loaded	group.Second_Lane_Loaded	Length - Span 1 (ft)	LLDF One Lane Net - Span 1 (per ft) (1)	LLDF Both Lanes Net - Span 1 (per ft) (1)	Support Location (ft)	LLDF One Lane Support 2 (per ft) (1)	LLDF Both Lanes Support 2 (per ft) (1)	Span Length 2 (ft)	LLDF One Lane Span 2 (per ft) (1)	LLDF Both Lanes Span 2 (per ft) (1)	Support Location (ft)	LLDF One Lane Support 3 (per ft) (1)	LLDF Both Lanes Support 3 (per ft) (1)	Span Length 3 (ft)	LLDF One Lane Span 3 (per ft) (1)	LLDF Both Lanes Span 3 (per ft) (1)
	42	1	1	0	26.667	0.063	0.085	26.667	0.054	0.080	40.000	0.059	0.082	66.667	0.054	0.080	26.667	0.063	0.085
	42	2	0	1	26.667	0.022	0.074	26.667	0.028	0.066	40.000	0.023	0.070	66.667	0.028	0.066	26.667	0.022	0.074
	42	3	1	1	26.667	0.043	0.080	26.667	0.041	0.073	40.000	0.041	0.076	66.667	0.041	0.073	26.667	0.043	0.080
	156	1	1	0	26.667	0.051	0.071	26.667	0.038	0.063	40.000	0.047	0.067	66.667	0.038	0.063	26.667	0.051	0.071
	156	2	0	1	26.667	0.019	0.071	26.667	0.024	0.063	40.000	0.020	0.067	66.667	0.024	0.063	26.667	0.019	0.071
	156	3	1	1	26.667	0.035	0.071	26.667	0.031	0.063	40.000	0.033	0.067	66.667	0.031	0.063	26.667	0.035	0.071
	216	1	1	0	26.667	0.051	0.071	26.667	0.037	0.063	40.000	0.046	0.067	66.667	0.037	0.063	26.667	0.051	0.071
	216	2	0	1	26.667	0.020	0.075	26.667	0.025	0.067	40.000	0.020	0.071	66.667	0.025	0.067	26.667	0.020	0.075
	216	3	1	1	26.667	0.035	0.073	26.667	0.031	0.065	40.000	0.033	0.069	66.667	0.031	0.065	26.667	0.035	0.073

Figure 7.3 Spreadsheet linking SlabDF and BrR

Summary											
	Analysis Strip, in	Span 1		Support 2		Span 2		Support 3		Span 3	
		1 lane	2 lanes	1 lane	2 lanes	1 lane	2 lanes	1 lane	2 lanes	1 lane	2 lanes
LLDF (Exterior) per ft	12	0.0635	0.0797	0.0539	0.0735	0.0594	0.0763	0.0539	0.0735	0.0635	0.0797
LLDF (Interior) per ft	12	0.0506	0.0713	0.0368	0.0627	0.0459	0.0672	0.0368	0.0627	0.0506	0.0713
LLDF Exterior Strip	60	0.3175	0.3983	0.2697	0.3673	0.2971	0.3817	0.2697	0.3673	0.3175	0.3984
LLDF Interior Strip	120	0.5063	0.7135	0.3675	0.6271	0.4593	0.6720	0.3675	0.6271	0.5064	0.7135

Figure 7.4 Spreadsheet linking SlabDF and BrR

							BrR LRFR
BrR Input Schedule Edge Strip (S1) (LRFR)							
Support Number	Start Distance	Length	End distance	Distribution Factor			Data Used for which spans
	ft	ft	ft	1 lane	1 Lane x 1.2	Multi-lane	
1	0.000	15.996	15.996	0.317	0.381	0.398	1
1	15.996	18.664	34.660	0.270	0.324	0.367	2
1	34.660	24.000	58.660	0.297	0.356	0.382	2
1	58.660	18.664	77.324	0.270	0.324	0.367	3
1	77.324	15.996	93.320	0.317	0.381	0.398	3

Figure 7.5 Spreadsheet linking SlabDF and BrR

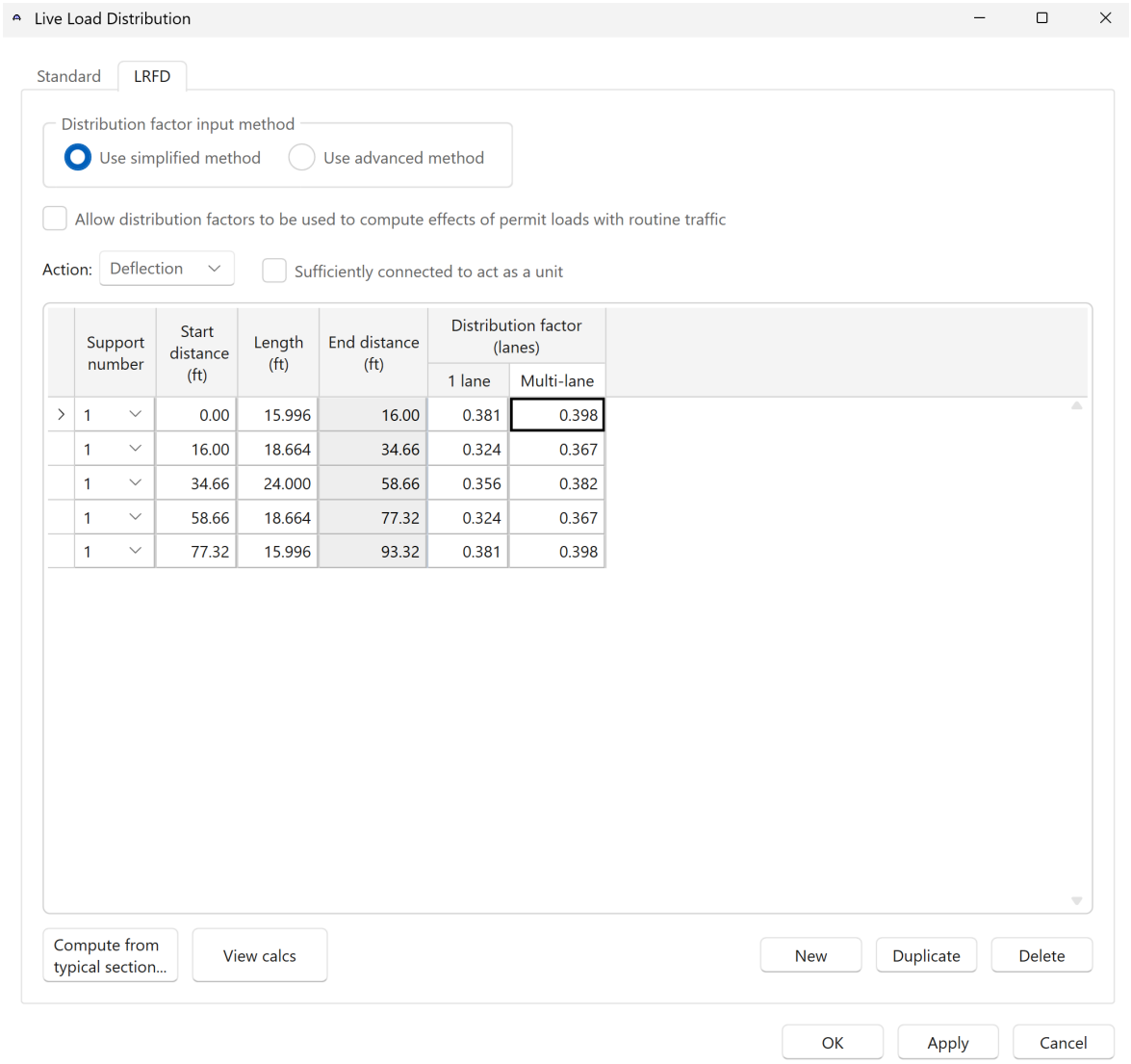

Figure 7.6 Spreadsheet linking SlabDF and BrR

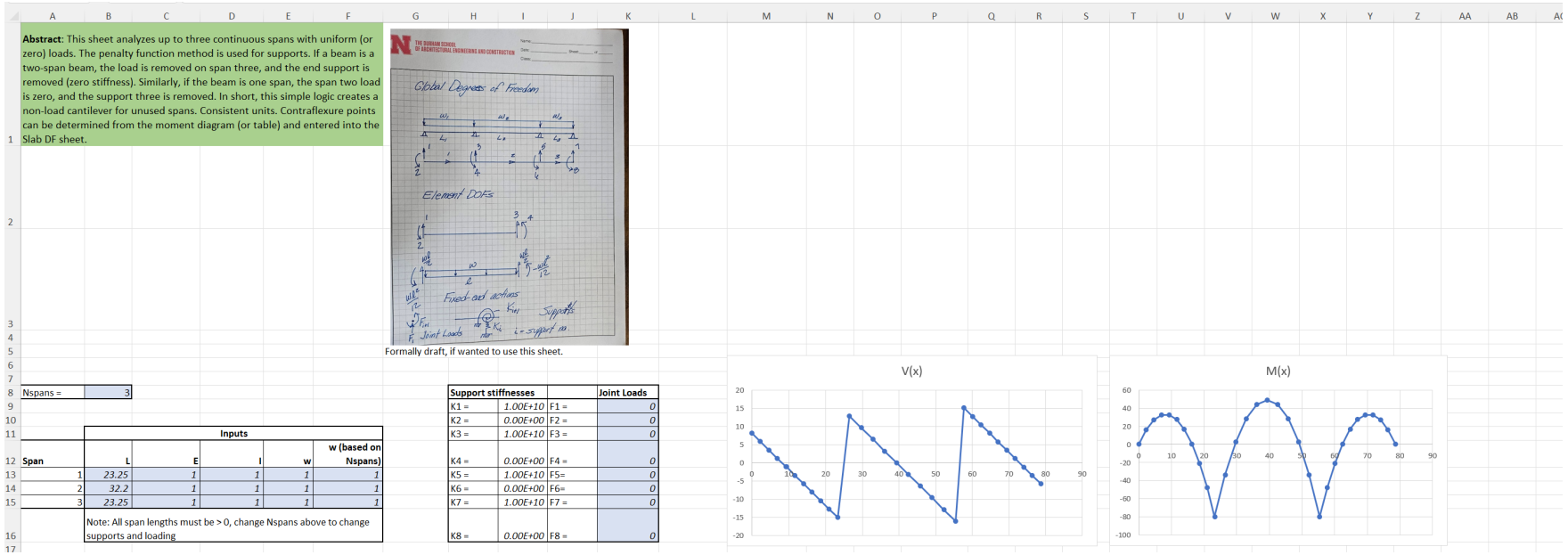

Figure 7.7 Beamline analysis for uniform load

Chapter 8 Summary and Conclusions

SlabDF was developed to support NDOT rating engineers in analyzing slab bridges. Based on a parametric definition, an FEA shell analysis was programmed for bridges with up to and including three spans. Bridges with more than three spans can be appropriately modeled with three-span substructuring.

A UI was developed based on the inputs and outputs from the base structural model. Outputs include 3-D graphics, 2-D graphics, and tabular data in both detailed and summarized formats. Support applications were developed to provide a simple beamline analysis for equilibrium moments and reactions, and for inflection points required for BrR. The team worked closely with NDOT engineers to develop an Excel spreadsheet to link the SlabDF results with BrR.

One example was written with a detailed narrative that provided inputs, outputs, methods of checking results, and interpretation of results. This example is included in the body of the report. Other examples are provided in appendices for two- and three-span bridges, a comparison bridge with SAP2000.

The project provides NDOT engineers with a tool that can be used in conjunction with professional judgment to provide more accurate load rating results for inventory, operating, posting, and permit rating.

References

Azizinamini, A., Boothby, T. E., Shekar, Y., & Barnhill, G. (1998). Bridge rating through field testing of reinforced concrete slab bridges. University of Nebraska–Lincoln / NDOR.

Conner, S., & Huo, X. S. (2006). Influence of parapets and aspect ratio on live-load distribution. Journal of Bridge Engineering, 11(2), 188–196.

Dymond, B., Hill, K., Hedegaard, D., & Linderman, R. (2023). New methods to determine safe bridge loading using field testing and refined analysis. Minnesota DOT / University of Minnesota.

Eom, J., & Nowak, A. S. (2001). Live load distribution for steel girder bridges. Journal of Bridge Engineering, 6(6), 489–497.

Harris, D. K., et al. (2021). Performance Characteristics of In-Service Bridges for Enhancing Load Ratings: Leveraging Refined Analysis Methods. Virginia Transportation Research Council, Report No. 21-R20.

Hill, K. (2022). Load Rating of Concrete Slab-Span Bridges. Master's Thesis, University of Minnesota.

Hill, K., Dymond, B., Hedegaard, D., & Linderman, R. (2022). Effects of barriers on load distribution in a concrete slab-span bridge. ACI Structural Journal, 119(4), 151–163.

Iowa DOT. (2008). Summary of Recent Bridge Research. Iowa Department of Transportation, Ames, IA.

Ravazdezh, F., Ramirez, J. A., & Haikal, G. (2021). Improved live load distribution factors for use in load rating of older slab and T-beam reinforced concrete bridges. JTRP Report FHWA/IN/JTRP-2021/06, Purdue University.

Smith, M., Eriksson, W., Shield, C., & French, C. (2005). Field and Laboratory Study of the Mn/DOT Precast Slab Span System. Minnesota DOT Report.

Zokaie, F. (2000). AASHTO-LRFD live load distribution factors. Journal of Bridge Engineering, 5(2), 131–138.

Appendix A One-Span Validation

NDOT Simple Span Validation 2025-04-28(NDOT_SimpleSpanValidation2025-04-28.pdf)

Appendix B Two-Span Validation

NDOT Two-Span Validation 2025-04-28(NDOT_Two-SpanValidation2025-04-28.pdf)

Appendix C Three-Span Validation

NDOT Three-Span Validation 2025-04-28(NDOT_Three-SpanValidation2025-04-28.pdf)

Appendix D Three-Span validation with SAP 2000™

NDOT Three-Span Validation with SAP 2025-05-06(NDOT_Three-SpanValidation_withSAP_2025-05-06.pdf)

Appendix E Mesh Studies

Mesh Studies – 2025-02-19(MeshStudies2025-02-19.pdf)